FERMILAB-TM-2436-APC

Original, February 17, 2009
Last update, March 26, 2010

Effect of Vacuum Condition on Performance of HINS RFQ

Henryk Piekarz

Accelerator Physics Center, FNAL

The arrangement of RFQ vacuum system is briefly described and projections of the vacuum level based on the standard out-gassing rates for the RFQ major components are compared with measurements. The permeation of water through the Viton O-rings of the LCW manifold inside the RFQ vacuum vessel is analyzed and compared with the RGA data. A possible origin of hydrocarbons emission into the RFQ vacuum space during the initial period of the RF power application is presented. A model where the out-gassing water from the vanes surfaces gives rise to parasitic currents during the RF pulse is outlined and its predictions are compared with the observed RFQ resonant frequency down-shift. The effect of temperature on the stability of the Inconel seals at the joints of the RFQ quadrants is described and the way to correct these joints is proposed. A model of the RFQ vacuum degradation due to open connection to the ion source and LEBT systems and possible improvement are presented. Effect of vacuum condition on the HINS RFQ beam transmission is discussed, and recommendations to bring the HINS RFQ to a status of proper operation are presented.

Contents: **Page**

1. Brief overview of the RFQ vacuum system 3

2. Expectations for the RFQ vacuum 3

3. Permeation of water through the Viton seals of the RFQ 8

4. Leak from RF couplers space into RFQ vacuum space 11

5. Out-gassing in the RFQ vacuum space with RF power 12

6. H_2O out-gassing from the vanes and the RFQ performance 14

6.1 Temperature rise at the RFQ vanes with instantaneous and average RF power 14

6.2 Formation of $[H_3O]^+$ and $[OH]^-$ ions on the RFQ vanes surface and the pressure rise in the RFQ vacuum space 16

6.3 Parasitic currents in the RFQ vanes vacuum space as potential source of the resonant RF frequency decay 19

7. Inconel seals of the vanes and their effect on RFQ operation 23

8. RFQ heat conditioning options 25

9. Spill of the ion source hydrogen gas into the RFQ vacuum space 28

10. Vacuum properties and beam transmission in HINS RFQ 30

11. Effect of ambient temperature on the RFQ vacuum 31

12. RFQ performance with repaired Inconel seal 33

13. Recommendations for improvement of HINS RFQ 34

14. Summary and conclusions 35

References 37

1. Brief overview of the RFQ vacuum system

As indicated in figure 1, RFQ consists of accelerating vanes made of solid copper embedded in a cylindrical (0.46m diameter x 3 m length) vacuum vessel of stainless steel. On the top of the vessel there are two 6 inch ports for the HV lines providing the RF power to the vanes, and two 8 inch ports for the LCW cooling flow of these vanes. At the bottom of the vessel there are three 10 inch ports for the vacuum pumps. On the vessel sides there are twelve 2-3/4 inch ports, for the RF signal pick-up, and four 2-3/4 inch ports for the vacuum instrumentation (Pirani Gauge, two Ion Gauges and the RGA). All ports on the vacuum shell use CF flanges with copper seals. The large front and back flanges of the vessel are sealed using the Viton O-rings. The Viton O-ring seal is also used in 24 feed-through lines to pick-up the RF signal, and in 48 VCO fittings of two LCW manifolds mounted at the top of the vessel interior.

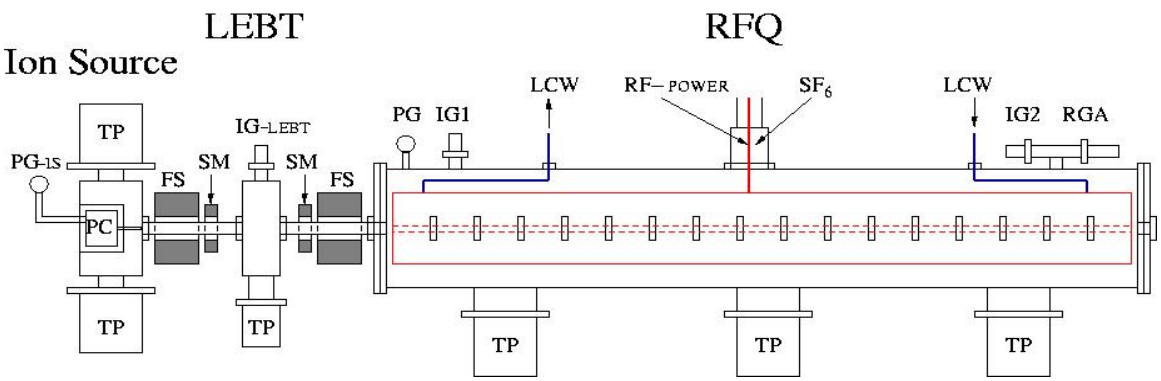

Fig.1 Arrangement of RFQ vacuum system with its connection to Ion Source through LEBT. PC- plasma chamber, FS- focusing solenoid, SM- steering magnets, PG- Pirani gauge, IG- ion gauge, TP- turbo pump.

All turbo pumps are Varian TV-1001 Navigator with the exception of the LEBT pump which is TV-301 type. The hydrogen gas pumping speed of the TV-1001 is 900 l/s while that of the TV-301 is 200 l/s. The Ion Gauges are the Granville-Phillips, Bayard-Alpert Nude 274 type, and the RGA is the Extorr 200 gas analyzer.

2. Expectations for the RFQ vacuum

The RFQ cross-section is shown in figure 2. The body of RFQ vanes constitutes a nearly closed object with small orifices through-out the center of the vanes as well as in their front and back flanges (not shown for clarity) to allow passing the accelerated beam. The pumping from the interior of the vanes is primarily through the15 slots, each 0.95 cm x 4.14 cm of cross-section and 2.20 cm in depth, evenly spread along the length of each quadrant. It is technically not possible to have a vacuum ion gauge inside the vanes space, so the vacuum level there has to be determined using an extrapolation of a measurement outside the vanes into the interior of the vanes. The conductance of the slot can be precisely calculated due to its regular and simple shape, but the conductance of both the interior and the exterior of the vanes is more complicated and will be estimated only. Due to very small dimensions of the slot, however, its conductance is by more than an order of

magnitude smaller than that of a neighboring space in the either interior or exterior of the vanes, and therefore primarily determining the overall conductance. This makes the estimating the conductance in all other spaces of the RFQ acceptable. This is especially true for the determination of the relative conductance of the various gas species which does not depend on the geometry of the vacuum system. At the end we will use the actual RFQ vacuum measurements to normalize, if needed, the projected both total and relative conductance for various gas species.

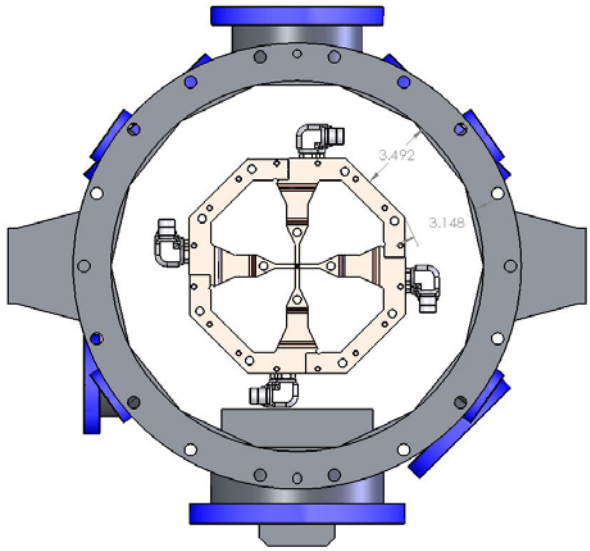

Fig. 2 RFQ cross-section: copper vanes are in the center of the stainless steel vacuum vessel. The shown bottom and top ports are for a turbo pump and the LCW connection, respectively. The placement of fraction of fittings of the LCW manifold is also shown.

We divide the molecular path in the interior and exterior of the vanes into sections so the conductance in each of them can be approximated using the formula for the cylindrical or the rectangular tube [1]:

Cylindrical tube: $C = \frac{1}{4}\, 478\, (T/300)^{1/2}\, (28/M)^{1/2}\, \pi R^2\, [1 + 3/8\, L/R]^{-1}$ (1)

Rectangular tube: $C = \frac{1}{4}\, 478\, (T/300)^{1/2}\, (28/M)^{1/2}\, ab\, [1 + 3/8\, (a + b)L/ab)]^{-1}$ (2)

T – temperature (K), M –atomic mass, R – radius of the pipe,
L – length of the pipe, a and b dimensions of a squared pipe cross-section

The selected sections are: (1) – space between two neighboring slots of vane interior, (2) – vane slots, (3) – space between RFQ body and vacuum shell, and (4) – entry into the turbo pump. The conductance is calculated for H2 and H2O, two major out-gassing species from steel and copper, and for N2, O2, CO, CO2, C3H8 and SF6 which represent air and other gases that can be potentially present in the RFQ vacuum space. In addition, a conductance of the hydrogen gas spilled from the LEBT beam pipe into, and then through, the interior of the RFQ vanes is also estimated. Finally, we project the pumping speeds for the gases originating in the interior and/or the exterior of the RFQ

vanes, and then project the partial and the total pressures inside and outside of the RFQ vanes space, both without and with the hydrogen spill from the LEBT section.

The interior of the vanes is naturally divided into 4 quarters, and we approximate the molecular flow in each quarter with 3 separate flows in a cylindrical tube of a cross-section equal to that of a ¼ of the vanes interior, and of a path length equal to the ½ of 1/3 length of vanes (representing 5 neighboring slots) as the molecules reaching a slot from further distances can be neglected. The space in the exterior of the vanes is more irregular, but as conductance there is expected to be high due to a rather large distance between the walls of the vanes and the vacuum shell, we also approximate that space with a cylinder of a cross-section equal to that of the total area between the vanes surface and the vacuum shell. As the pumps are symmetrically distributed along the RFQ vacuum shell we use the geometrical sum of a ½ distance between the RFQ ends and a ½ of mean path from the top and the bottom rows of slots to the pumps as an average distance of the molecular flow. Again, this procedure leads to underestimation the overall conductance in the exterior space of the vanes. The assumed geometries of the RFQ vanes interior and exterior sections for the estimation of the conductance are listed in Table 1.

Table1. Assumed geometry of various sections of RFQ for conductance calculation

Section	<R> [m]	a [m]	b [m]	<L> [m]
¼ Vane within area of 5 slots	0.042	-	-	0.25
Vane slot	-	9.525 e-3	4.14 e-2	2.3 e-2
Vanes to vacuum shell space	0.19	-	-	0.7
Turbo pump entrance	0.1	-	-	0.1

The mass coefficients (¼ 478 $(T/300)^{½}$ $(28/M)^{½}$) for the selected gases at 10^0 C and 30^0 C are given in Table 2, and the summary of the estimated partial and total conductance for various gases emitted from the interior and the exterior of the RFQ vanes surfaces at 30^0 C is given in Table 3. The conductance from the interior of the RFQ, $C_{RFQ\text{-}INT}$ is defined as:

$$1/C_{RFQ\text{-}INT} = 1/C_{VANES} + 1/C_{SLOTS} + 1/C_{VAC\text{-}SPACE} + 1/C_{TP} \qquad (3)$$

The conductance from the surfaces outside the RFQ vanes (including vacuum shell) is defined as:

$$1/C_{RFQ\text{-}EXT} = 1/C_{VAC\text{-}SPACE} + 1/C_{TP} \qquad (4)$$

The C_{VANES} is a sum of the conductance in 4 vanes, and the C_{SLOTS} in all 60 slots.

Table 2. Mass coefficients for conductance calculation

Gas specie	H2	He	H2O	N2	O2	CO	CO2	C3H8	SF6
Coefficient @ 10^0 C	1736	1228	579	464	435	464	414	414	207
Coefficient @ 30^0 C	1877	1328	626	502	470	502	448	448	224

Table 3. Estimated partial and total conductance for various gases in the RFQ

RFQ COMPONENT	Conductance [L/S]						
	H2	He	H2O	N2 / CO	O2	CO2/ C3H8	SF6
Inner vane, 1/3 length	804	569	269	215	201	192	96
1 slot	87	62	29	23	22	21	10
Space outside vanes	22310	15785	7440	5968	5586	5323	2655
Turbo pump inlet	3430	2427	1144	918	859	818	408
Inner vanes to pumps	3269	2312	1090	875	819	780	389
Outside vanes, or vac. shell to pumps	7046	4985	2350	1885	1764	1680	839

The pumping speeds, $S_{RFQ\text{-}INT}$ and $S_{RFQ\text{-}EXT}$ are projected using the equation (5) for the interior and the equation (6) for the exterior of the RFQ vanes (this one includes also vacuum shell) where S_{TP} is the nominal pumping speed of all three turbo pump:

$$1/S_{RFQ\text{-}INT} = 1/S_{TP} + 1/C_{RFQ\text{-}INT} \quad (5)$$

$$1/S_{RFQ\text{-}EXT} = 1/S_{TP} + 1/C_{RFQ\text{-}EXT} \quad (6)$$

We apply the nominal 900 L/s pumping speed of hydrogen in TV-1001 Varian pump to all other gases. This is certainly incorrect as the pumping speed for the heavier gases is likely 20 % lower, but in the absence of data we have no other choice. This assumption, however, is valid as long as hydrogen remains a dominant gas as expected.

Table 4. Projected pumping speed for various gases emitted inside and outside vanes

RFQ COMPONENT	Pumping Speed [L/S]						
	H2	He	H2O	N2 / CO	O2	CO2/ C3H8	SF6
Inside vanes space	1479	1245	776	660	628	605	340
Outside vanes space	1952	1750	1256	1110	1067	1036	640

In order to project the vacuum level in the RFQ we must know the surface areas of the vanes and the vacuum shell, and we have to assume the out-gassing rates. The surface areas were very precisely determined [2] using a solid modeling analysis, but the

assumptions of the out-gassing rates is rather uncertain. Nevertheless this exercise is useful as at a very minimum it helps understand relative contributions of the different gas species emitted from various areas of the RFQ internal structure.

The RFQ has been pumped and remained under vacuum for many months now. The vacuum state, however, was interrupted multiple times to allow installation of RF couplers and some instrumentation. During these periods a pure nitrogen gas was purged through the RFQ system. The out-gassing rates are very strong function of the surface quality (e.g. machined versus polished) and cleanliness that may effectively change those rates by orders of magnitude. As we have no knowledge of the way the RFQ surfaces were prepared we assumed standard out-gassing rates for the clean but unbaked surfaces of stainless steel and copper after 100 h of pumping as reported in [3]. We note, however, that typically warm vacuum level is stabilized with a minimal rate of gas desorption only after some 100-200 days of pumping.

The most common gases emitted from the stainless steel and the OFHC copper are hydrogen (57%), water (37%), and CO + CO2 (6%) with the out-gassing rates from the copper being typically factor 2 higher than those from the steel. The RFQ RGA mass spectrum shown in figure 3 provides an evidence of that with a striking exception that the

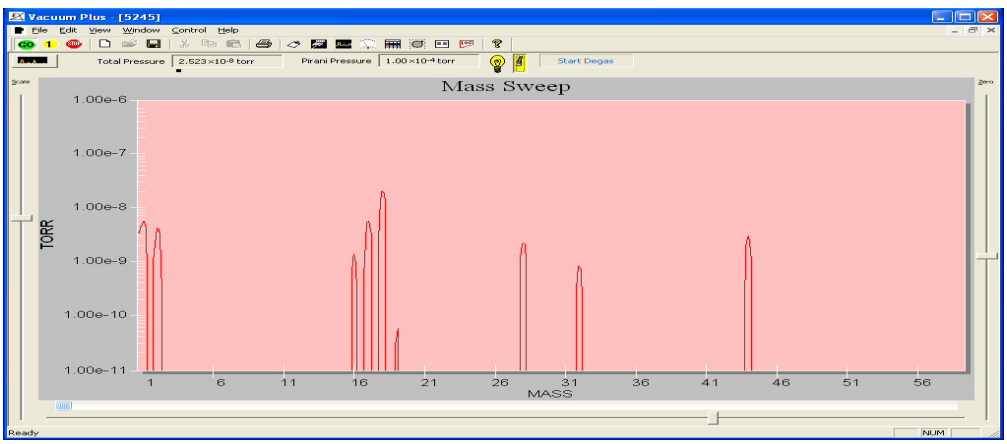

Fig. 3 RGA mass spectrum at 16^0 C with RF couplers filled with air (H_2-> M=2, H_2O -> M =16-19, N_2/CO -> M= 28, O_2 -> M=32 and CO_2 -> M=44)

relative rate of water to hydrogen is much higher than expected. As the pumping goes on the relative rate of H2O should get smaller and the hydrogen will become dominant gas specie. Using these assumptions we made projections for partial and total pressures inside and outside spaces of the RFQ vanes. The surface areas of the copper and steel, the assumed out-gassing rates for the H2 and H2O, and the projected partial and total pressures are given in Table (5). Partial pressures inside the vanes, $P_{RFQ\text{-}INT}$, and outside the vanes, $P_{RFQ\text{-}EXT}$, are calculated using the equations (7) and (8), respectively:

$$P_{RFQ\text{-}INT} = C_{RFQ\text{-}INT} / S_{RFQ\text{-}INT} \qquad (7)$$

$$P_{RFQ\text{-}EXT} = C_{RFQ\text{-}EXT} / S_{RFQ\text{-}EXT} \qquad (8)$$

Table 5. Projected partial and total pressures of H2 and H2O in the RFQ vacuum spaces

	Units	Inside Vanes		Outside Vanes			
Material		Cu		Cu		SS	
Area	[m^2]	7.14		2,47		4.73	
Gas Species		H_2	H_2O	H_2	H_2O	H_2	H_2O
Outgassing Rate	[Torr_L/S/m^2]	$1.3\ 10^{-6}$	$8.6\ 10^{-7}$	$1.3\ 10^{-6}$	$8.6\ 10^{-7}$	$6.7\ 10^{-7}$	$4.3\ 10^{-7}$
Outgassing	[Torr_L/S]	$9.3\ 10^{-6}$	$6.1\ 10^{-6}$	$3.2\ 10^{-6}$	$2.1\ 10^{-6}$	$3.2\ 10^{-6}$	$2.0\ 10^{-6}$
Pumping Speed	[L/S]	1479	776	1952	1256	1952	1256
Partial Pressure	[Torr]	$6.3\ 10^{-9}$	$7.9\ 10^{-9}$	$1.6\ 10^{-9}$	$1.7\ 10^{-9}$	$1.6\ 10^{-9}$	$1.6\ 10^{-9}$
Total Pressure	[Torr]	$1.4\ 10^{-8}$		$0.7\ 10^{-8}$			

We observe that projected pressure inside the vanes is twice that of the outside one. This is due to both the assumed double out-gassing rate for the copper and a smaller conductance from the interior of the vanes to the pumps. The projected pressure outside the vanes is $0.7\ 10^{-8}$ Torr to be compared to the measured ones with IG1 and IG2 ion gauges at $1.5\ 10^{-8}$ Torr with RF couplings uninstalled and the LCW water not flowing in the vanes cooling channels. At the time this measurement was conducted the IG readings still continued to fall. Therefore, we view this comparison as satisfactory, and as a vindication of the assumptions used for estimation of the conductance as well as for the out-gassing rates. In this situation we are not introducing any "normalization" factor for the further analysis of the RFQ vacuum system.

3. Permeation of water through the Viton seals of the RFQ

Although the RFQ vacuum system was intended to operate in a UHV range there is rather a large number of Viton O-ring seals used. The list of these Viton seals is given in Table 6. In Table 7 we present permeation factors [4] of various gases in Viton O-rings

Table 6. Length of RFQ Viton seals

Location	OD [inch]	Mean Length [mm]	Count	Total Length [cm]
LCW Manifold	0.625 0.75	50 75	32 4	160 30
Total LCW Manifold				190
Vacuum Shell	18 0.375	1466 30	2 10	293 30
Total Vacuum Shell				323
Total RFQ				513

relative to helium at 20^0 C and at 1 bar differential pressure. We also show the actual permeation value for air [5] under the same conditions. The permeation strongly depends on the temperature, e.g. it typically (but varying with gas specie) increases by a factor of two from 20^0 C to 40^0 C [4], and for well soluble gases it rises linearly with a rise of the differential pressure.

Table 7. Relative permeation of gases through Viton (20^0 C, 1 bar differential pressure)

Gas Specie	He	H2O	H2	N2	O2	CO2	Ar	Air
Relative Permeation	1	23	0.2	0.047	0.13	0.16	0.13	0.065
Permeation per Linear Inch of Ring								$1.5\ 10^{-8}$ Torr-L/S

For a total of 202 inch length of Viton rings in the RFQ vacuum vessel we expect ~ $3\ 10^{-6}$ Torr-L/S of air permeation rate. With the projected air pumping speed of 1100 L/S in the outer space of the vanes air permeation would then contribute about $2.7\ 10^{-9}$ Torr pressure to the RFQ vacuum. As the actual vacuum was measured to be ~ $1.5\ 10^{-8}$ Torr the air permeation constitutes less than 20% of the RFQ vacuum level. The air permeation factor given in [5] is for a free-standing Viton ring. In the vacuum chamber, however, Viton rings are placed inside the grooves, which if properly designed and machined, allow for a complete closure of the mating halves of the flange, and in this way strongly minimizing the effective permeation rate. In order to determine the strength of this effect we will use the detection of helium from the permeating air performed under the same conditions. The helium flow rate from air was measured using a very sensitive (7.510^{-12} Torr-L/S, Alcatel Model 182 leak detector, and it was found to be $4.8\ 10^{-11}$ Torr-L/S. As there is 5 ppm of helium in the air at atmospheric pressure we can project the permeation rate of air to be:

$$\text{Perm (air)} = 2\ 10^5 \times 0.065 \times 4.8\ 10^{-11} = 0.6\ 10^{-6}\ \text{Torr –L/S} \qquad (9)$$

Comparing this result with the air permeation prediction of $3\ 10^{-6}$ Torr-L/S based on data from [5] we find that in the RFQ vacuum system the permeation of air through Viton seals is suppressed by about a factor of 5. Using this suppression factor (1/5) we can estimate the permeation rate for the water vapor through the Viton rings of the LCW manifold. As the water circulates under 3 bar pressure we add additional factor 3 and a factor of 0.38 for the LCW manifold fraction of all RFQ Viton seals:

$$\text{Perm (H2O)} = 1/5 \times 3 \times 0.38 \times 10^6 \times 23 \times 4.8\ 10^{-11} = 2.5\ 10^{-4}\ \text{Torr-L/S} \qquad (10)$$

With the H2O estimated pumping speed of 1256 L/S in the outside vanes space we project then the partial pressure due to H2O permeation to be: P (H2O-perm) = $2.0\ 10^{-7}$ Torr. As shown in figure 4, within few minutes after the LCW flow has begun in the LCW manifolds the vacuum level has risen to about $2.1\ 10^{-7}$ Torr. As the initial reading

(IG1) was ~ 2.5 10^{-8} Torr the excess pressure caused by the LCW flow is ~1.85 10^{-7} Torr, thus being in an agreement with the expectation.

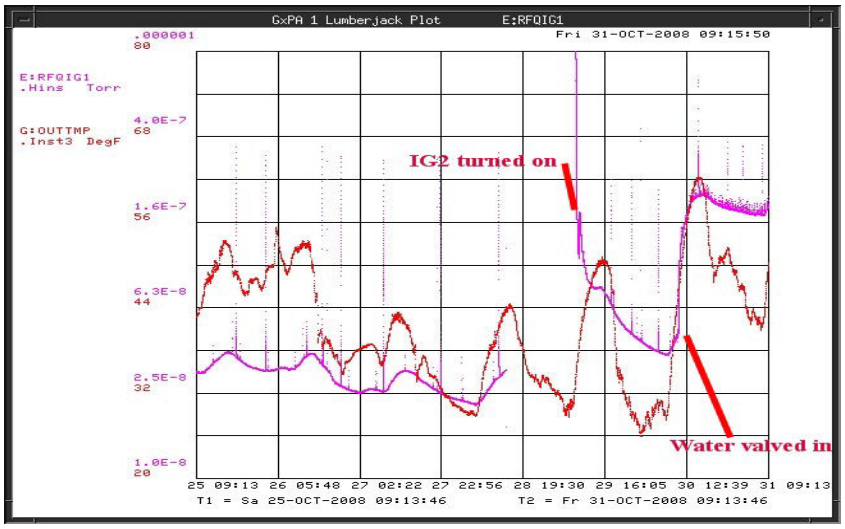

Fig. 4 Pre-LCW flow RFQ vacuum level (IG1), and vacuum level rise (IG2) with LCW flow

The LCW manifold is outside of the vanes structure so the water vapor spreads into the internal space of the vanes primarily through 60 slots with a total H2O conductance of 1740 L/S. As the conductance in the outside space of the vanes is 7440 L/S we expect that only some 23% (1740/7440) of these water molecules enter the inner space. The water molecules which got inside the vanes space bounce between the walls as other molecules from the out-gassing process, and then they are pumped-out at 776 L/S rate. Due to a very high solubility of water molecules in copper (typically twice of that in the stainless steel), however, a considerable fraction (perhaps (1740 – 776)/1740 = 55%)) of these "external" H2O molecules will actually stick to the inner vanes surfaces and "refill" the outer molecular layers of copper with water.

The most direct evidence of water permeation through the Viton rings was found during the operation of connecting the Ion Source and LEBT to the RFQ. After these systems were connected the RFQ vacuum pumping was not re-started for about 2 days in order to allow for the mechanically undisturbed alignment of the IS/LEBT to the RFQ. During the alignment process, however, the LCW water continued to flow through the RFQ vanes. When the RFQ vacuum pumps were turned on after the completion of the alignment a small flow of water was observed at the outlets of all 3 fore-pumps as shown in figure 4. In the absence of the vacuum pumping the permeated LCW water from the manifold has been condensing on the much colder RFQ vacuum shell inner surface and then stored in the bottom of the vessel. When the fore-pumps were turned on this water was pulled out through the turbo pumps (not working yet) into the outside world. After this incidence the water was purged out of the manifold. It was very interesting to observe that the relative RFQ vacuum level with and without LCW water in the manifold (4.6 Torr / 16.6 mTorr) corresponds nearly exactly to the relative permeation of water and air through the Viton O-rings.

Fig. 4 Paddle of water that exited from the RFQ fore-pump

4. Leak from RF couplers into RFQ vacuum space

There are two RF couplers mounted on the top of the RFQ vacuum shell. Their HV connections use ceramics joints to isolate from the ground potential. The main body of the coupler is sealed to the vacuum shell with a CF flange, but there are also O-rings used to seal the coupler's pressurized protective gas (N_2 or SF_6). If the soldered joint of the coupler ceramics fails than this gas will leak into the RFQ vacuum space. Up to now either air or nitrogen gas was inside the RF couplers. When the coupler is filled with air both N_2 and O_2 masses are observed in the RGA (figure 3), and when the air was replaced with nitrogen only the N_2 mass is seen (figure 5). In figure 5 there is also a very strong presence of the hydrogen gas. This is due to hydrogen spill from the Ion Source and LEBT sections into the RFQ vacuum space after the opening of the isolation valve. The absence of any indication of air (no oxygen mass) suggests there is no air leak into the LEBT or Ion Source vacuum chambers.

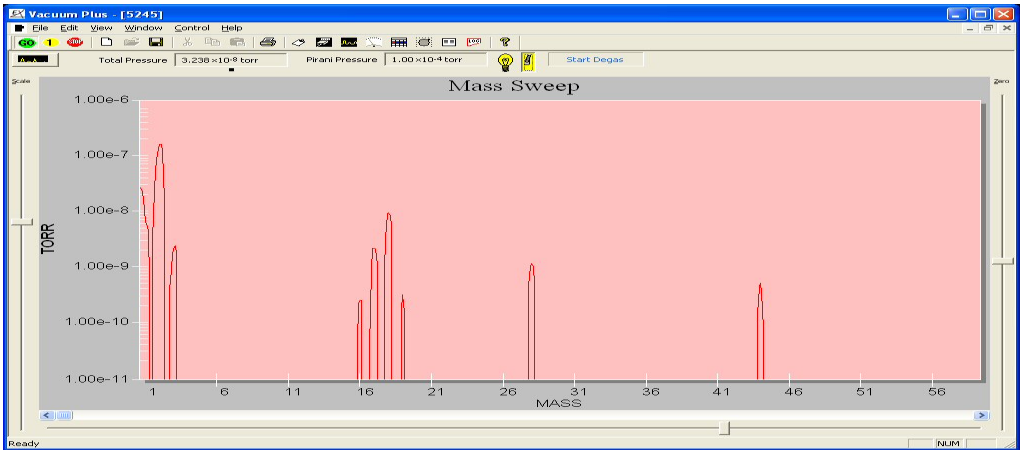

Fig. 5 RGA spectrum with nitrogen gas in the RF coupler (no oxygen mass) at 16^0 C

5. Out-gassing in the RFQ vacuum space with RF power

We observe that at the onset of the RF power application the RFQ vacuum level gets much higher (up to a factor 10) and the RGA mass spectrum gets much broader with the gas masses ranging up to 44 and even above, as shown in figure 6. As the RF power

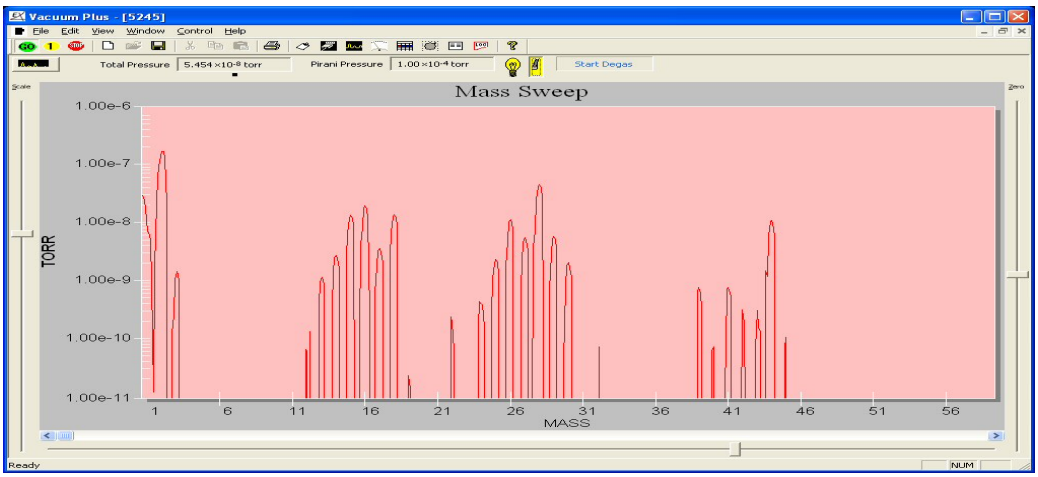

Fig. 6 RGA mass spectrum at the beginning of the 20 W averaged RF power application

continues, however, the emission of these heavy masses subsides, and it may not be as high when after a short break the RF power is raised again. This is contrary to the water associated masses for which the emission remains high even after a longer period of the applied RF power, as illustrated in the subsequent figures 7, 8 and 9. The heavy masses

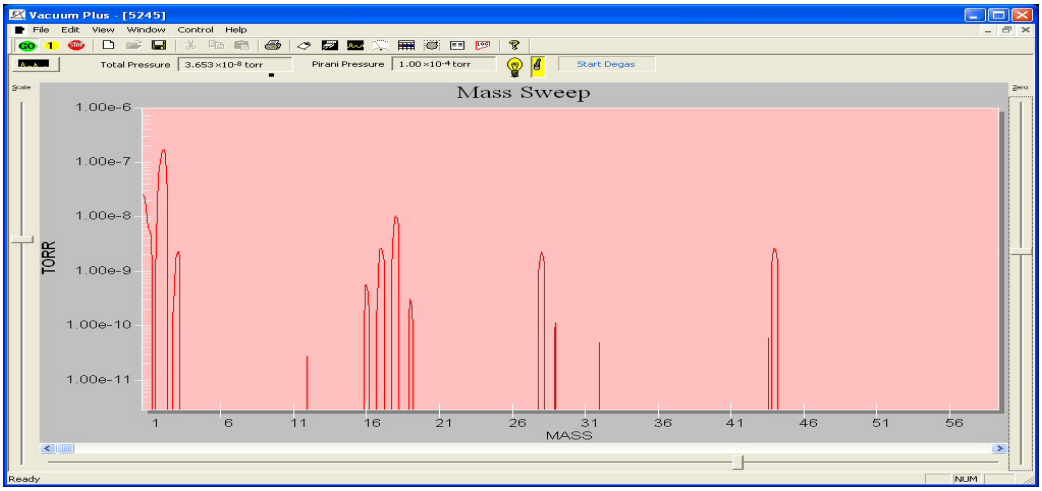

Fig. 7 RGA mass spectrum after few hours of 20 W averaged RF power application

are naturally attributed to hydrocarbons. As they are not observed, however, without the RF power they do not result from the standard out-gassing of the RFQ inner components.

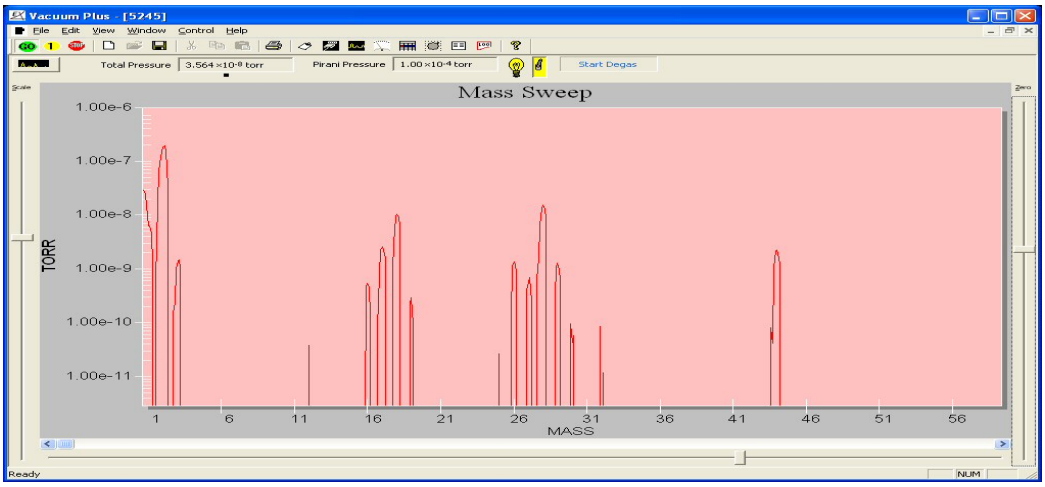

Fig. 8 RGA mass spectrum at the beginning of 40 W averaged RF power application

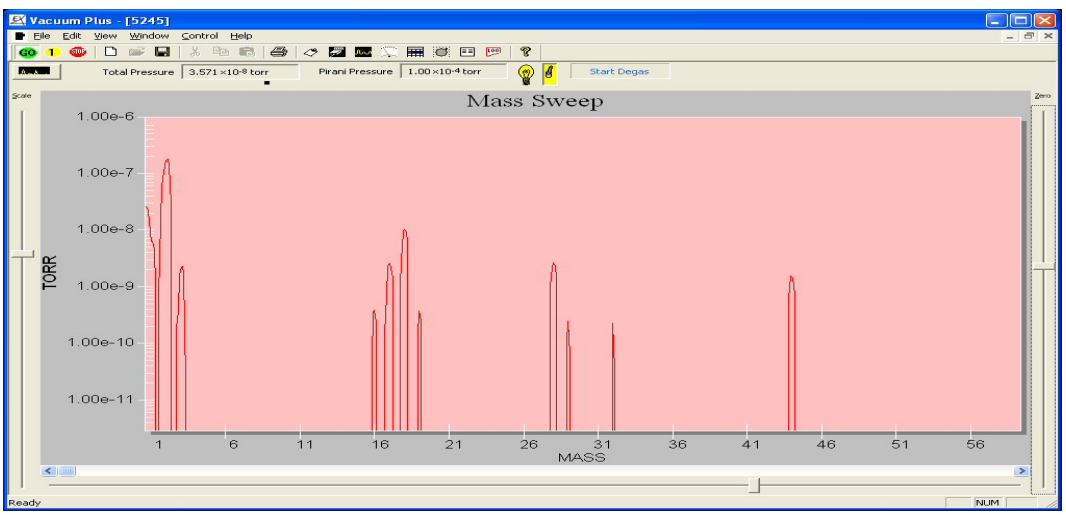

Fig. 9 RGA mass spectrum after few hours of 40 W averaged RF power application

The RF power provides HV and heating to the surface of the RFQ component but it's the heating that will induce the out-gassing. The most heating occurs at the vanes tips but the OFHC copper used to construct the RFQ can not be the source of hydrocarbons. There are many RF power monitoring cables inside the RFQ vacuum space and so their insulation could be the source. The problem with this hypothesis is that these cables do not heat-up with the RF power. So if the hydrocarbons were out-gassing from the cables insulation they should be also observed without the RF power.

The above analysis brings us to a suggestion that the RFQ RF coupler is the source of the hydrocarbons. We know that a solder is used to seal the coupler's HV tip and the effect of sparking was indeed observed on the tip during the coupler repair for the vacuum leak. The solder uses rosin core to help producing a good electrical contact at the soldered joint. The rosin core is an organic compound construct of large and complex

hydrocarbon molecules. If these molecules get onto the surface they will break-down in the HV field to smaller but charged molecules giving rise to sparking and observation in the RGA. As the application of RF power continues fewer and fewer rosin core molecules remain on the surface and the sparking subsides. The rosin core molecules are very large and so their drift from the bulk of the tin into the surface is slow even under the pulling force of vacuum. After some period of time in the absence of the RF power induced heating they will migrate to the surface and become the source of the sparking again. The emission of hydrocarbons into the RFQ vanes space produces the unwanted sparking and it may also lead to the increase of the multipacting by ionization electrons. But as their appearance subsides while the RF power is applied they should allow for the RFQ operation after certain "conditioning" period.

6. H_2O out-gassing from the vanes and RFQ performance

6.1 Temperature rise at the RFQ vanes surface with instantaneous and average RF power

The HINS RFQ has been designed to operate with instantaneous RF power of 450 kW. The acceptable maximum average RF power, however, is 4500 W with various possible combinations of the pulse lengths and repetition rates as long as the duty factor does not exceed 1%. Consequently, the HINS proposal assumes the RFQ operations with e.g.:1 ms pulse at 10 Hz, or 3.5 ms pulse at 2.5 Hz. We show below, however, that within the applied range of repetition rate the RF pulse length constitutes much more important qualifier for the RFQ performance than the average RF power.

In the earlier HINS RFQ tests (where the effect of "running away" RF frequency was discovered) the performance was investigated using the average RF power ranging from 300 W up to1200 W. The instantaneous power of (325-400) kW in the 3.5 ms long RF pulse was used requiring repetition rates of 0.25 to 1 Hz. In the tests after the RFQ repair the pulse of 1 ms length was used with the repetition rate of 2 Hz producing 650 W of average RF power deposited in the RFQ. Typically the temperature rise of the RFQ is estimated by depositing the averaged RF power into the entire RFQ body. This temperature rise is countered with the heat removal through the LCW cooling water flowing through the channels in the RFQ body, as indicated in figure 7 [6]. The characteristic temperature distribution due to 3 kW average RF power shown in figure 7 indicates only a marginal temperature rise (fraction of a Kelvin) at the vanes tips (furthest away from cooling water channels). If this was true than for any practical purpose the RF power induced heat would not affect RFQ performance.

The RF power, however, does not act directly on the whole RFQ body mass. At 350 MHz the RF power affects only about 3.5 μm thick skin of the RFQ body. So with 3 kW (equivalent to a 3 kJ/s) of an average RF power the entire volume of the RFQ skin (3.5 e^{-6} m x (7.14 + 2.47) m^2 = 34 cm^3, 0.3 kg mass) will heat-up by:

$$(3\ \text{kW}/400\text{J/kg-K}) / 0.3\ \text{kg} = 25\ \text{K} \qquad (11)$$

As indicated in figure 7 this temperature rise, however, is suppressed about 30 times, down to 0.8 K at the vanes tips, as a result of the heat transfer to the larger RFQ body in

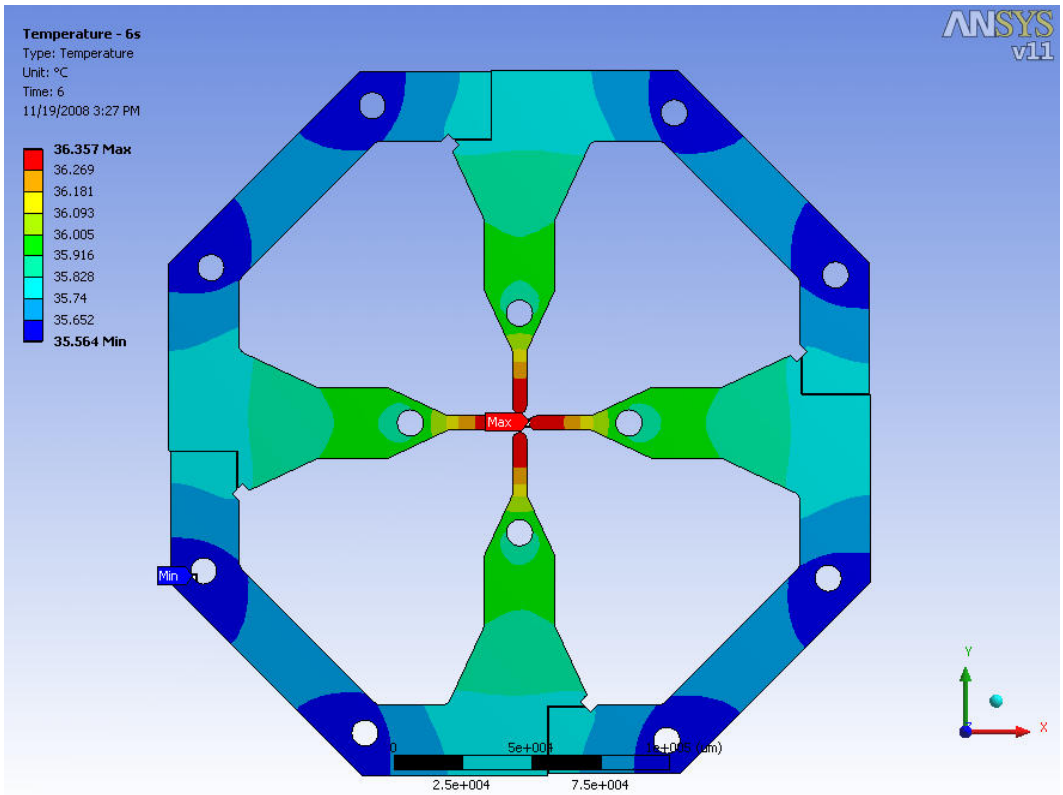

Fig. 7 RFQ temperature profile with applied average RF power of 3 kW

combination with cooling provided by the LCW flow channels. The temperature profile shown in figure 7 was obtained assuming that the average RF power is the acting heating power of the RFQ body but the instantaneous temperature rise of the RFQ skin during the RF pulse is certainly much higher. As the power of the micro RF pulse is constant the average RF power is a combination of the macro pulse length and its repetition rate. During the macro pulse which is typically 1-4 ms long neither the heat transfer to RFQ body nor the LCW cooling can be very effective. Consequently, for e.g. a 3.5 ms long RF pulse the momentarily temperature rise at the vanes tips is expected to increase to 230 K, as indicated in equation (12):

$$1\text{s} / 3.5\ e^{-3}\text{s} \times 0.8\ \text{K} = \sim 230\ \text{K} \qquad (12)$$

(and ~ 66 K for the 1 ms long RF pulse) if the heat transfer and LCW cooling are ignored. The heat transfer to the larger RFQ body, however, slows down the temperature rise even within the short RF pulse. At the room temperature the heat transfer in copper is ~ 1 cm^2/s (or10^8 $\mu m^2/s$) allowing for the heat to spread up to 10 skin depths during the 3.5 ms pulse and up to 5 skin depths with 1 ms pulse. The heat is mostly concentrated, however, in the outer skin which is directly affected by the RF power. If the heat concentration was linear with respect to the affected total depth of the RFQ vanes the temperature rise at the

outer skin would be reduced to 46 K with 3.5 ms pulse and 26 K with 1 ms pulse. The heat distribution is more likely exponential suggesting even higher temperature rise in the outer layers of RFQ vanes. The residence time of water molecules decreases by an order of magnitude with each 20^0 C temperature rise [3]. Consequently, the possibility that with 3.5 ms pulse the momentarily temperature rise of the vanes surface is by 20^0 C higher than with the 1 ms pulse, suggests that the water out-gassing rate with the longer pulse may be by as much as an order of magnitude stronger than with the shorter pulse.

6.2 Formation of $[H_3O]^+$ and $[OH]^-$ ions on the RFQ vanes surfaces and pressure rise in the RFQ vacuum space

As high electric field (30 MV/m) is used to accelerate particles in the RFQ it is common to observe sparking in the RFQ vacuum space. This sparking is typically due to the ionization of contaminants (oil, water, etc.) on the RFQ surfaces when they are exposed to sweeping electric fields. The released ionization electrons when get into the areas of rather low electric fields will multiply through a multipacting process causing disturbance in RFQ operation. These effects, however, usually diminish to an acceptable level after conditioning of the RFQ with a bake-out and also by running at low RF power for a certain period of time. In the case of the HINS RFQ, however, a different problem was encountered. It turns out that as the application of the RF power continues the RF frequency is more and more unsustainable, and at some point in time the loss becomes very dramatic making RFQ operations impossible. Below we outline a model where the water out-gassing from the vanes surfaces of the HINS RFQ explains the RFQ malfunctioning. Specifically the model shows that the onset time for the rise of both the vacuum level and the reflected RF power frequency loss occur almost exactly at the same time, as it is in fact observed.

As the out-gassing of water constitutes ~ 90% of all molecules in the HINS RFQ vacuum space the molecular properties of water play dominant role in determination of the vacuum level. With no RF power the RFQ vacuum level is in the range of (2-4) 10^{-8} Torr (depending on the ambient temperature), and at the RF power of 600 W pressure raises to (3-5) 10^{-7} Torr [7]. In this pressure range the vacuum is characterized by a molecular flow where molecules jump multiple times on the surface from one location to another before reaching inlet to the pump, the RGA or the ion gauge. The residence time at each point on the surface can be very long depending on the molecule type and the temperature of the surface. For the water molecules the residence time on the metal surface at 22^0 C is about 10^5 seconds. In addition, water molecules are internally polarized which causes a strong affinity between them leading to creation of $[H_2O]^2$ clusters which can also reside long time on the surface further delaying vacuum gauge response. Consequently, with the out-gassing water being a strongly dominant gas in the HINS RFQ the RF induced heating does not change much the vacuum level until a larger portion of the vanes surfaces is covered at least with a monolayer of H_2O molecules.

In the absence of strong electric or magnetic fields the $[H_2O]^2$ clusters may undergo only a spontaneous chemical reaction of self-ionization (11):

$$[H_2O] + [H_2O] \rightarrow [H_3O]^+ + [OH]^- \quad (11)$$

These ions also recombine almost as quickly as they are produced so their concentration is extremely low (one pair of ions per 5.6 10^8 water molecules).The reaction (11) very strongly intensifies, however, if the electric field is present. A cartoon-like view of the ion pair formation and subsequent emission from the metal surface in the presence of high electric field is shown in figure 8. First the electric field re-orients hydrogen atoms

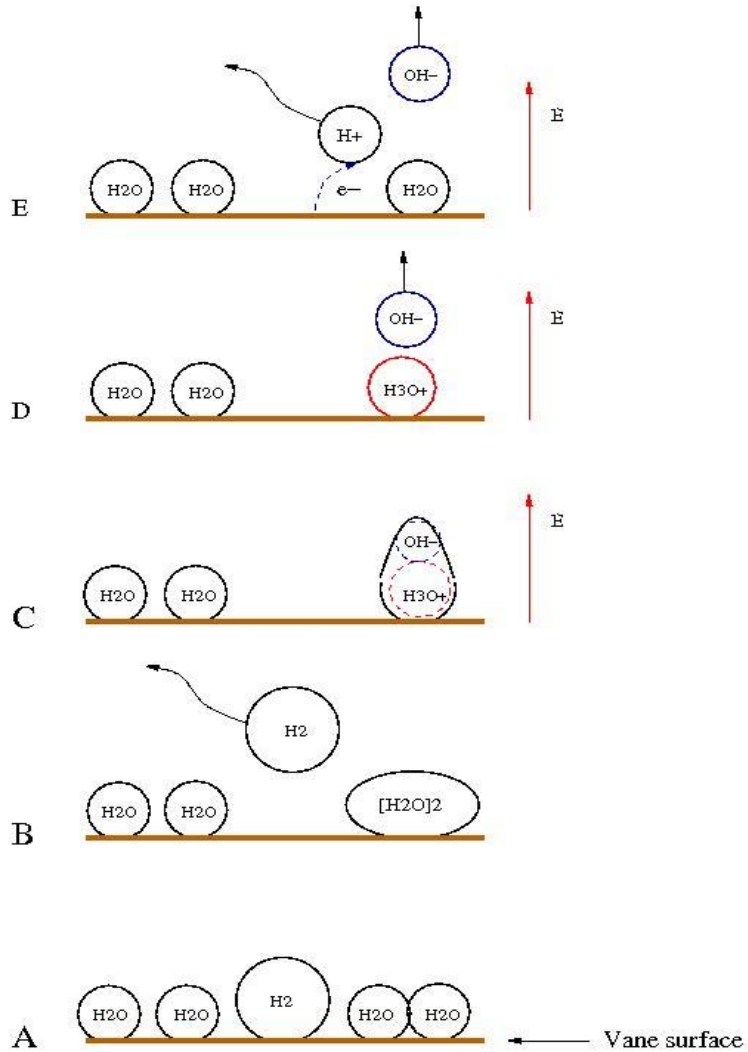

Fig. 8. A cartoon illustration of $[H_2O]^2$ cluster formation and break-up into $[H_3O]^+ + [OH]^-$ ion pair on the metal surface: A – Out-gassed H_2 and H_2O molecules on the vane surface, B – H_2 molecule detaches from the surface and drifts into the vacuum space while the neighboring H_2O molecules form $[H_2O]^2$ cluster, C - $[H_2O]^2$ cluster aligns with the electric field E, D- Polarized $[H_2O]^2$ cluster separates into $[H_3O]^+$ and $[OH]^-$ ion pair under high electric field E, and E – $[H_3O]^+$ acquires electron from the metal surface and breaks into H_1 and H_2O molecules while the $[OH]^-$ ion drifts along the E-field lines.

in the water molecule toward the electrodes facilitating formation of a dog-bone like cluster aligned with the E-field. Then at the onset field E_0 (in the range of MV/m) they

are torn apart creating $[H_3O]^+$ and $[OH]^-$ ions pair. In this high electric field the $[H_3O]^+$ ion quickly acquires electron from the metal surface, and then instantly breaks to H_1 and H_2O neutral molecules ($[H_3O]^+ + e^- \rightarrow H_2O + H_1$). The negative OH^- ions on the other hand can't be easily neutralized and with the mass of 17 amu they move rather slowly in the electric field remaining near the metal surface for a very long time.

The onset E-field has been a subject of many studies, e.g. [8]. For technical reasons these studies are performed using the ice water at very low temperatures. Formation of water ice on the metallic surface allows predetermine the number of H_2O molecular layers, and as the ice stays put in the vacuum a detection of emerging ions from the ice surface is technically possible. It turned out that the E_0 field is very strongly temperature dependent changing by about a factor of 100 between 120 K and 220 K [8]. We observe that in the RGA spectrum of the RFQ vacuum the mass peak of 19 amu is indeed observed (figure 8), if the overall water level is sufficient. As this ion mass can only be due to the $[H_3O]^+$ ions this observation indicates that the reaction 11 occurs within the RGA space. Knowing the HV (15-30 kV/m) and the temperature (370-390 K) range of the RGA filament we get an important data point in addition to those reported in [8]. In order to cope with the large change of the E_0 value with temperature we plot in figure 9 $\ln E_0$ (T) rather then E_0 (T). In fact, a linear extrapolation [8] would lead to a non-physical conclusion, that virtually no electric field would be needed to break the $[H_2O]^2$ clusters into the ions even at the water temperatures well below freezing. Our plot, however, is arbitrary, and its sole purpose is to indicate a possible range of the E_0 values at the RFQ operational electric fields and temperature.

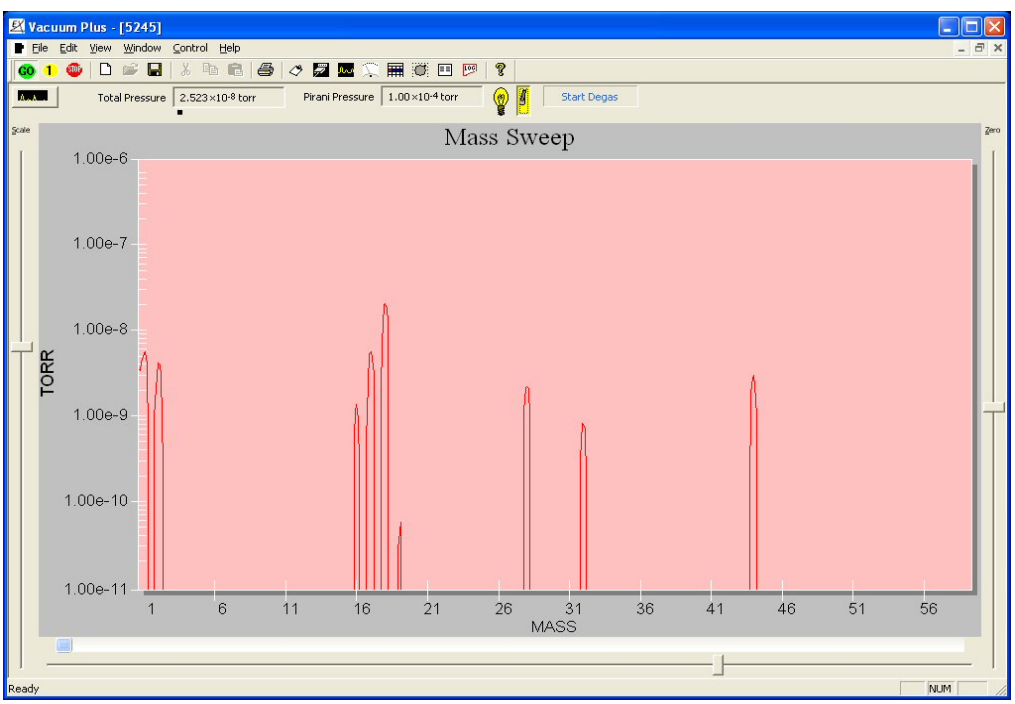

Fig. 8 RGA spectrum showing mass 19 in addition to 16, 17and 18 masses due to water molecules

The maximum E-field at the HINS RFQ is about 33 MV/m but as indicated in figure 9 it fades away (as a sine function) to a near zero value at the bottom of the vanes cavity.

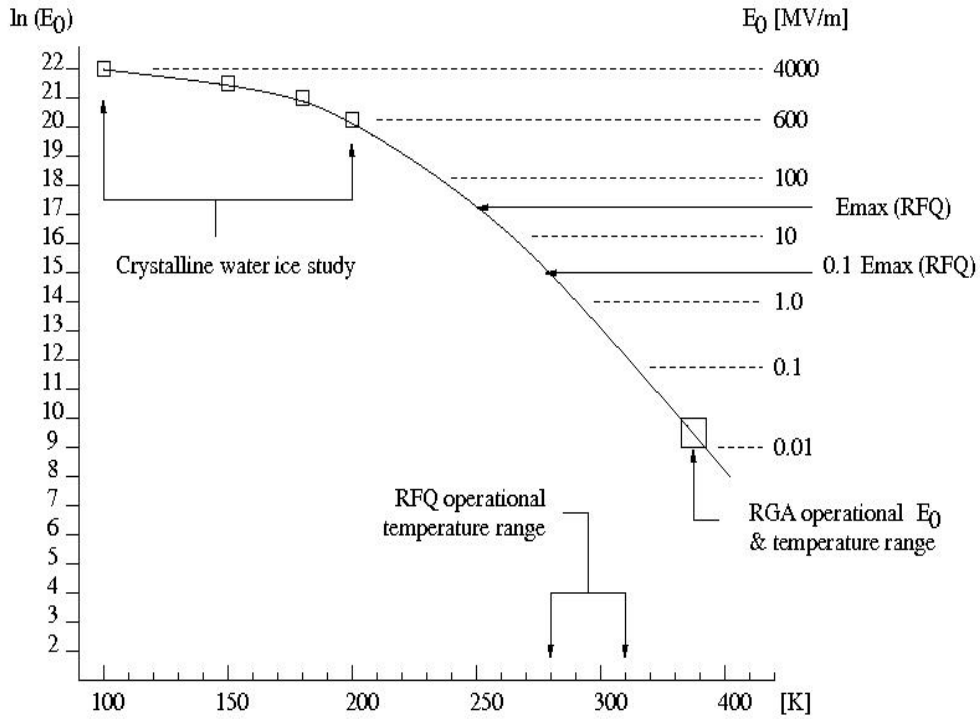

Fig. 9 Onset E-field for the $[H_2O]^2 \rightarrow [H_3O]^+ + [OH]^-$ as a function of temperature

6.3 Parasitic currents in the RFQ vacuum space of RFQ vanes as potential source of the resonant RF frequency decay

Based on the analysis and observations presented in 5.1 it is reasonable to assume that the E-field on all surfaces of the RFQ vanes tips is certainly strong enough to break the $[H_2O]^2$ clusters into the ion pairs (eq. 11) at the room temperature. It is also interesting to note that the high frequency mode (350 MHz) of the RFQ operation facilitates both the formation and the tearing apart of the $[H_2O]^2$ clusters in the same (or just the next one) pulse, and therefore making this process very efficient. A simplistic view of the RFQ vanes cross-section with indications of the E-field inside vanes cavity and along the beam path is shown in figure 10. A possible drift path of the $[OH]^-$ ions in the space between the RFQ vanes is shown in figure 11. The drifting ions induce current on the vanes surface altering in this way the electric field profile and potentially inducing the RF power loss. As this parasitic current increases the ability of the RF power supply to compensate for the power loss is more and more suppressed and forcing it at some point to step-down its resonant frequency. So, the question is: Are there enough H_2O molecules on the vanes surface as a result of the RF power induced heating to allow for a significant formation of $[H_2O]^2$ cluster and so leading in this way to the creation of the parasitic $[OH]^-$ ion currents?

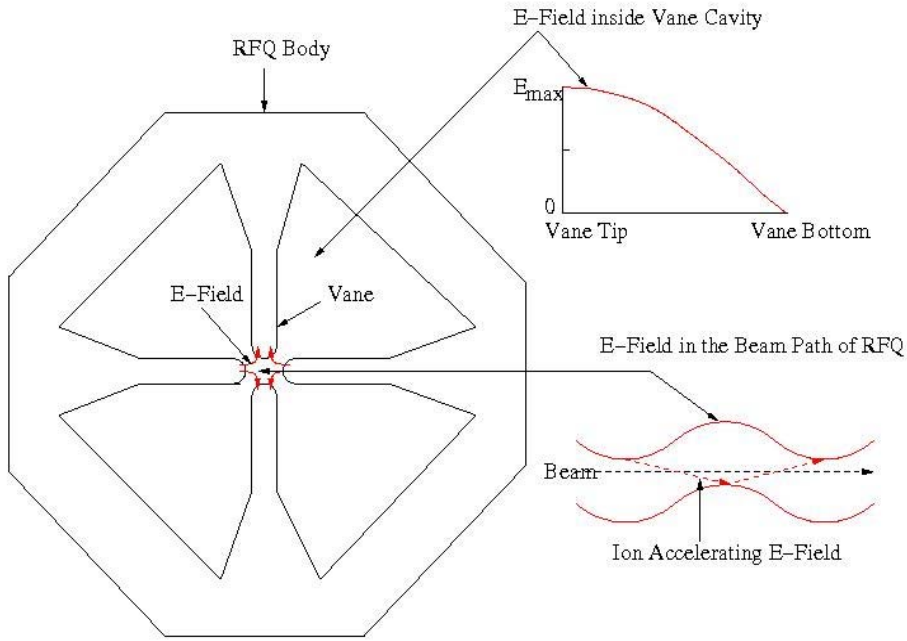

Fig. 10 RFQ vanes cross-section with indication of the E-field inside vane cavity and along the beam path

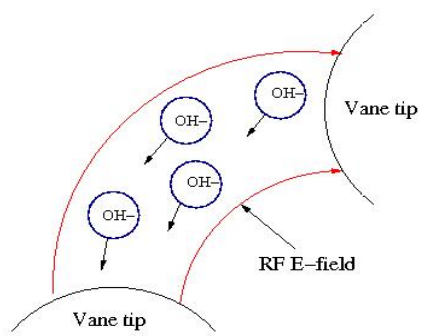

Fig. 11 Drift of $[OH]^-$ ions along the RF induced E-field lines between the vane tips

We observe that application of a 600 W RF power to the RFQ increased the vacuum level from ~ 2 10^{-8} Torr to ~ 3 10^{-7} Torr. Using the RGA measured ratio of H_2O/H_2 ~ 9, and the H_2O molecular conductance from the internal to the outer vanes spaces (see Chapter 2), we project that the H_2O out-gassing rate, O(H_2O_600W), in the internal RFQ vanes spaces has risen to ~ 1.9 10^{-5} Torr_L/s/m^2, as given by the equation (12):

$$O(H_2O_600\ W) = [0.9 \times 3\ 10^{-7} \times (1256/776)] / [(2.0 \times 10^{-8})] \times 8.6\ 10^{-7}\ \text{Torr_L/s/m}^2 \quad (12)$$
$$= 1.9\ 10^{-5}\ \text{Torr_L/s/m}^2$$

The rate of the H_2O molecules appearance on the surface of the RFQ vanes is then:

$$N_{H2O} = 6\ 10^{23} \times 1/18g \times 0.8g/L_atm \times 1.9\ 10^{-5}\ Torr_L/s_m^2 \times 1/760\ atm/Torr \quad (13)$$
$$= 6.5\ 10^{14}\ molecules\ /\ s_m^2$$

And for all inner vanes surface (7.14 m^2) the rate of H_2O molecules appearance is:

$$N_{H2O}\ (RFQ\text{-}inner\ surface) = 4.6\ 10^{15}\ molecules\ /\ s \quad (14)$$

As discussed earlier the vane tips are the most prone to the RF induced heating and therefore probably responsible for most of the observed pressure rise. With the vanes tips area (red and yellow in figure 9) of about 6000 cm^2 the appearance density of the H_2O molecules on the vanes tips is then:

$$N_{H2O}\ (RFQ\text{-}tips) = (7.14\ m^2 / 0.6\ m^2) \times 4.6\ 10^{15}\ molecules\ /\ s_tips \quad (15)$$
$$= 5.5\ 10^{16}\ molecules\ /\ s_\ tips$$

In order to compare this density to the H_2O molecular size we present it (16) per nm^2:

$$N_{H2O}\ (RFQ\text{-}tips_nm^2) = 5.5\ 10^{-2}\ molecules\ /\ s_nm^2 \quad (16)$$

The H_2 and H_2O molecules diameters are 0.47 nm and 0.28 nm, respectively. So, the hydrogen molecules occupy considerably more space per molecule on the surface. However, if the out-gassing of hydrogen relative to water is nearly suppressed (which is the HINS RFQ case) 14 single H_2O molecules are needed to cover 90% of a 1 nm^2 of the vane surface. Consequently, for the case of 600 W RF power the minimum time required for a formation of a single molecular H_2O layer on the vanes tips is:

$$(14\ molecules/\ nm^2) / (5.5\ 10^{-2}\ molecules\ /\ s_nm^2) = 250\ s \quad (17)$$

In reality this time is much longer because many molecules out-gassed from the tips will jump out and settle on the colder surfaces of the vanes before reaching the ion gauge long before the filling of the tips surface is fully complete. If the all inner surfaces of the vanes would have to be covered with the H_2O monolayer the required time would be:

$$(7.14\ m^2 / 0.6\ m^2) \times 250\ s = 2970\ s \quad (18)$$

As all the vanes surfaces are affected at some level by the RF induced heating the actual time to fill the tips area with the H_2O monolayer is somewhere between 250 s and 2970 s, but probably much closer to the lower limit as the vane tips areas are the main out-gassing source. It turns out that the observed time with the 600 W RF power is about 720 s thus matching well our projected time range.

At this point if the RF power continues the formation of a second water molecular layer begins, and the RF high electric field gives rise to production of the $[H_3O]^+$ and $[OH]^-$ ions which in turn generate a parasitic current. If all clusters on the vanes tips were100 % ionized then following the equation (19) an average current of ~ 0.018 A would be generated:

$I_{[H2O]2}$ (RFQ-tips) = [5.5 10^{16} molecules /s_tips] / [3.12 10^{18} charges/s] = ~ 0.018 A (19)

The RF power, however, is applied with a duty factor of 1% so this parasitic current is generated in the 0.01 second time period being in fact a pulse current of 1.8 A. Probably only a fraction of the ions will drift and be accelerated in the vanes E-field as many of them are neutralized when hitting the surface even at the first time. Nevertheless this parasitic current which naturally shows as a reflected RF power is likely to be high enough to alter the RFQ electric field profile which gets worse and worse as the RF power continues. The heating power of the parasitic ion current scales as $(I_{parasitic})^2$, and therefore with the increase of the RF average power e.g. by factor 2 the onset time for the RF frequency fall is shortened by factor 4, which is exactly as observed in [7] (figure 12).

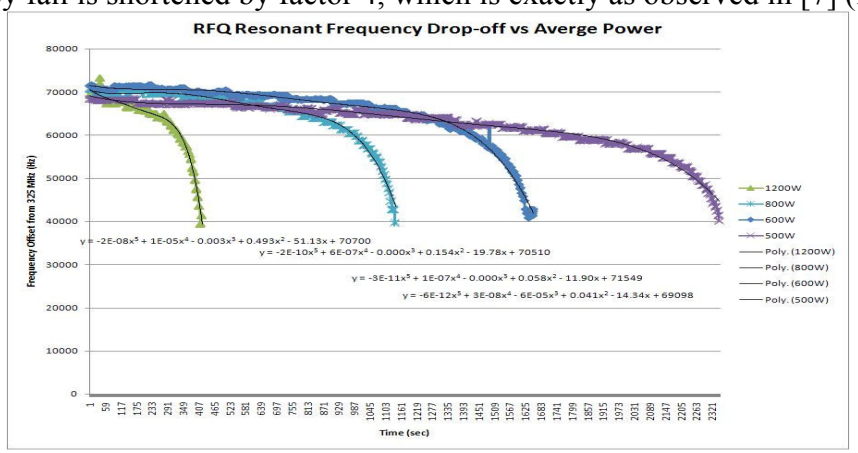

Fig. 12 RFQ resonant frequency fall for (from left to right) 1.2 kW, 0.8 kW, 0.6 kW and 0.5 kW. Vacuum rise which is almost mirror reflection of RF fall was not included in data graph.

We illustrate in figure 13 our model predictions for the offset of the RFQ frequency fall and the vacuum rise with 1.2 kW and 0.6 kW of average RF power. In our model the end

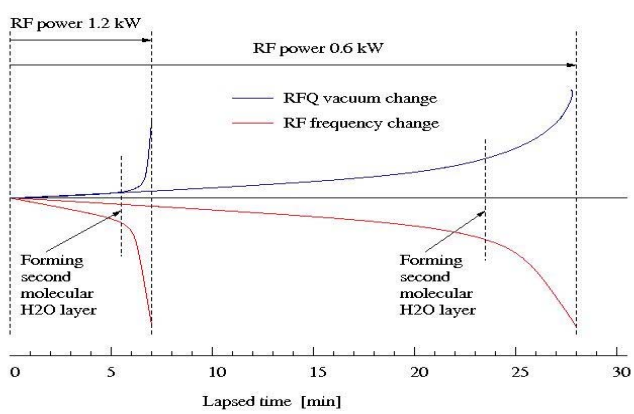

Fig. 12 Projected lapsed time to a rapid fall of RF frequency and to a rapid rise of vacuum level for average RF power of 0.6 kW and 1.2 KW

of the monolayer formation of water molecules on the vanes tips triggers a strong rise of both the vacuum level and the parasitic ion current. Both the vacuum level and the RF frequency offset should show rise, though at slower pace, from the beginning of the RF

power application because there will be always $[H_2O]^2$ clusters created on the vanes tips surface even at very low molecular density. Due to very high affinity of water molecules to the metal surface, however, the rate of rise of the vacuum level may be slowed down relative to that of the RF frequency rapid fall offset, a trend that is indeed observed [7].

It is important to note that if the out-gassing rate of water was much lower than that of hydrogen (as it should be in the water leak-free vacuum vessel after a long pumping period) hydrogen molecules produced as a result of the RF power induced heating would occupy most of the space on the vanes surfaces (especially during the RF pulse) and therefore strongly suppressing formation of water clusters.

7. Inconel seals of the vanes and RFQ operation

There are four seals between the quadrants of the RFQ. Their purpose is to provide electrical contact between the quadrants. We do not have RFQ manufacturer information about the seal material or its dimensions. We know, however, that the material used is Inconel. For this analysis we assume that it is Inconel-718, the most popular one for such applications. We assume that the seal is a copper-clad pipe of ~6.4 mm (~1/4") diameter and ~0.76 mm (~0.030") wall slit along the length. Each seal is composed of two pipes inserted butt to butt at the center. The Inconel has a very strong tensile strength and high elastic modulus. These properties allow the Inconel pipe to act as a spring when squeezed into the prepared groove between the RFQ vanes quadrants securing in this way good electrical contact. Some thermal properties of Inconel and copper at 20^0C are listed in Table 8 below:

Table 8. Thermal properties of Inconel-718 and OFHC copper (* estimated)

	Inconel	Copper
Specific heat, Cp [J/kg-K]	435	385
Thermal expansion, Texp [μm / m-K]	13.0	17.0
Thermal conductivity, Tcond [W / m-K]	11.4	401
Thermal diffusivity, Tdiff [cm^2/s]	0.029*	1
Density [g / cm^3]	8.19	8.96

The thermal expansion of copper is slightly higher than that of Inconel which means that in the heating/cooling processes the length of the vanes groove expands/shrinks more than the seal. As the seal is composed of 2 units, each ~ 1.5 m length, the expansion per unit seal has to be compared to that of the holding groove. This differential expansion is given in Table 9 below for the temperature increases of up to $\Delta T = 60$ K.

Table 9. Differential expansion of copper-Inconel on 1.5 m path

ΔT [K]	10	20	30	40	50	60
ΔL Inc [μm]	195	390	585	780	975	1170
ΔL Cu [μm]	255	510	765	1020	1275	1530
ΔL (Cu-Inc) [μm]	60	120	180	240	300	360

As just the ambient temperatures can change by 30 K (e.g. from 10^0C to 40^0C) there has to be a gap of more than 0.4 mm between the seal units, and a gap of more than 0.2 mm between the seal outer end and the RFQ flange. Based on information supplied by the manufacturer there is no free space left between the two sections of the seal. A visual inspection of the seal ends, however, indicates existence of about 1.5 mm gap to the RFQ inner flange. It is assumed that the thermal expansion forces are countered by the friction force resulting from the spring force of the slit Inconel pipe. This may allow drag the seals together with the expanding/shrinking vanes. One should not expect, however, the RFQ engineering design to count on that as the friction force is very unlikely to be uniform along the entire seal path. Consequently, even under a very moderate temperature change the seal sections may shift irreversibly, and lack of the gap between the seal sections may result in popping-up of the seal out of its groove.

In addition to the difference in the expansion between the copper and Inconel there is even more significant difference in the thermal diffusivity. We present Inconel thermal diffusivity in relation to that of the copper using the formula (21) below:

$$\text{Tdif_Inc} \sim \text{Tdif_Cu} \times [\text{Tcond_Cu}/\text{Tcond_Inc}]^{-1} \times [\text{Cp_Cu}/\text{Cp_Inc}]^{-1} \times [\rho\text{_Cu}/\rho\text{_Inc}]$$

$$\sim \; 1 \text{ cm}^2 / \text{s} \times [35.18 \times 1.13]^{-1} \times 8.96 / 8.19 = 0.029 \text{ cm}^2 / \text{s} \qquad (21)$$

The above result indicates that with the same heating/cooling power applied to the equal volumes of copper and Inconel it will take for the Inconel about 33 times longer (1/0.029) than for the copper to raise/lower the temperature by the same amount. As the seal is a hollow tube, the actual mass volume is about ~9 mm^2 x length as compared to a rod volume of ~ 32 mm^2 x times length. Therefore, the Inconel tube will warm-up (or cool - down) by about a factor of 3 faster than the plain rod but the small contact area (not larger than 30%) of the seal tube to the vanes surface eliminates this gain.

With the two-part seals both the heating and the cooling process opens a possibility of relative shifting and even popping-up the seals out of the vanes. Replacing the split-seals with the single seals matching the full length of the RFQ vanes will significantly meliorate the seal-vane assembly as far as the temperature changes are concerned.

The RFQ vanes seal cooling related problem may be helped by shutting down the LCW cooling flow after the RF power is stopped. The RFQ is placed inside the vacuum vessel, so there are two ways in which it is cooled-off. One is through the radiation heat transfer, and the second one is with the conductive heat transfer using the LCW water flow through its vanes. The radiation heat transfer is very slow for the objects placed in the vacuum, so in the absence of the conductive heat cooling of the vanes the RFQ body temperature will decrease very slowly as well. In such a case the much faster conductive heat transfer between the vanes and the seals will keep-up their temperatures at near equalization, even if their thermal diffusivities are much different.

The formula for the radiation heat transfer is given below:

$$Q = \varepsilon\, \sigma\, (T_h^4 - T_c^4)\, A \qquad (22)$$

where $\varepsilon = \sim (0.023 - 0.052)$ for the polished copper, $\sigma = 5.67\ 10^{-8}$ W/m^2_K, T_h and T_c are the object's "hot" and "cold" temperatures, and A is the object surface area. So, for the RFQ of 9.61 m^2 area the required radiation heat transfer to bring the temperature from 60^0 C down to 20^0 C, assuming the larger value of ε parameter is:

$$Q = 0.052 \times 5.67\ 10^{-8}\ (333^4 - 293^4)\ 9.61\ \text{W} = 140\ \text{W} \qquad (23)$$

In order to lower the 700 kg of RFQ copper mass by 1 K the energy of 2.7 10^5 J (or W-s) is required, so with the 140 W of radiation heat transfer it would take 1.93 10^3 seconds, or 32 minutes. If the RFQ body was heated up by 40^0 C then the time required to bring it back safely to a room temperature would be ~ 21 hours.

Application of the RF power requires the LCW water to flow through the RFQ vanes for the removal of the generated heat. This heat removal will lead to a mismatch of the vanes and seals temperatures during the cooling period after the RF power is stopped. There is a possible solution to this problem. The LCW flow should be tied to the RF power using a by-pass valve for the RFQ cooling manifold that gets closed for a period of time when the RF is applied, and gets open when the RF power is stopped. As the water will stay in the manifold at the same pressure as during the circulation and the water circulation continues in its purification circuit outside the RFQ, the followed-up closing of the bypass valve will not affect the LCW water cooling performance in the RFQ. An additional cross-check (and possibly a second safety system) for this operation will come from the temperature sensors placed on the RFQ main body.

8. RFQ heat conditioning options

The vanes seals arrangement described in Chapter 7 prevents application of heaters to the RFQ body in order to outgas its water. Removal of the water embedded in the metal surfaces using only the vacuum pumping is a very long-term process (months, if not years - see Recycler), if performed at the room temperature. Increasing the temperature by only 20 K is enough to increase the out-gassing rate by an order of magnitude. The minimization of the out-gassing rate of water from the vanes surfaces is most detrimental to achieve a proper performance of the RFQ. Therefore one should have the ability to heat-up the RFQ vanes at any time when required. If the RFQ remains "unused" for some period of time the water molecules embedded in the deeper molecular layers of the vanes surfaces will refill the "vacancies" at the surface and the new heat treatment will be required.

A successful RFQ operation was achieved in [9] only after a very intense RFQ body baking to 70^0 C combined with a very strong pumping system [10, 11] which included use of cryo-pumps. A recent RFQ commissioning effort at KEK [12] encountered similar problems to those of the HINS RFQ including loss of the RF power and very poor beam transmission. Their planned solution focuses on a significant improvement of the vacuum

system e.g. increase water pumping speed to 6900 L/S (this is 3 times of the HINS RFQ) and baking the RFQ body to 70^0 C. Using our model of the parasitic currents formation and the associated vacuum rise (Chapter 6.3) we present in Table 10 very arbitrary projections of the shortest lapsed time to the appearance of the resonant RF frequency fall as a function of the RFQ heating temperature and for two values of the RF average power. These lapsed times are strongly underestimated as the heating time at a given temperature and the length of the followed-up pumping period are not used in this estimation. In addition the longer heating times will certainly compensate for the use of lower heating temperature, probably in an order of magnitude range, but this can be only determined in a practical test. Nevertheless Table 10 clearly illustrates the importance of heating the RFQ body as well as the choice of the 70^0 C heating temperature in [9, 12].

Table 10. Projected shortest lapsed times to appearance of RF resonant frequency fall for the low and high RF average powers after RFQ heat treatment

RFQ Heating Temperature [^{0}C]	RF Average Power 650 W [hours]	RF Average Power 4500 W [hours]
30	1	0.02
40	3.3	0.2
50	10	0.6
60	33	1.8
70	100	6

The application of the tape heaters placed on the outside surface of the RFQ main body is a good solution for the HINS RFQ. A set of temperature sensors will provide control of both the temperature gradients and the temperature rate of rise as induced by the heaters. As long as the cooling-down of RFQ body is based on the radiation heat transfer (which it is when conducted in the vacuum and without LCW flow) there is no danger for occurring of a mismatch of the seal shrinkage versus the vanes shrinkage. The following arrangement is required for the heating/cooling of the RFQ body using SS tape heaters:

1. SS heater tapes to wrap available space on the outside of the RFQ – two unused 6” CF flanges can be used to house heater power cables
2. Two heater power supplies, each 2.5 kW
3. Temperature sensors (12 or more) on the outside surface of the RFQ – the unused 2 ¾” CF can be used to pass readout cables
4. RF power controlled solenoid valve(s) for the by-pass of the LCW flow in the RFQ vanes (such a valve probably exists on the RFQ already).

The application of hard heating (e.g. 70^0 C) requires use of single length Inconel seals. If the exchange of the 2-part Inconel seals with the single length ones is deemed too difficult at present one may apply much less drastic method of heating the RFQ body by using multiple cycles of purges RFQ vacuum space using heated-up nitrogen gas with followed-up high vacuum pumping. Such a method, however, is not a substitute for the hard heating as it will remove moisture only from rather a narrow layer of vanes surface.

Possible arrangement of the SS heater tape and the hot nitrogen purge are shown in figure 13. For the heaters we assume 2 scenarios: (1) heater tape is uniformly distributed on the entire RFQ body, and (2) the heater tape wraps only the end parts of the RFQ. Then second option is for the case when the 2-part Inconel seals are not replaced with the single ones and the repair of the LCW manifold is accomplished by sliding-out about ¼ of the RFQ length on each end allowing placing the heating tapes only in those sections.

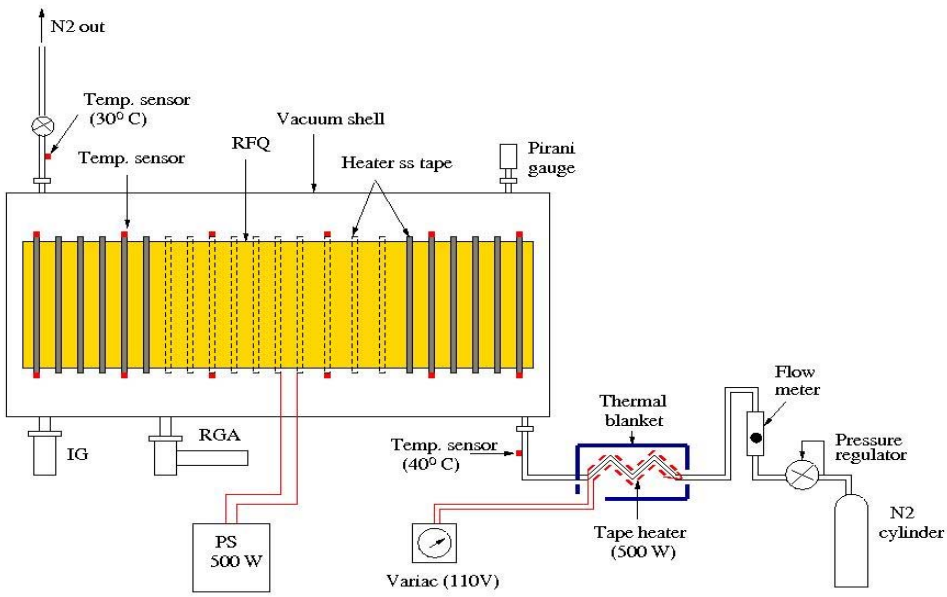

Fig. 13 Possible arrangements of tape heaters and/or hot nitrogen purge. The dashed lines indicate heater tape placement for a full RFQ body heating.

For the purging system using a combination of both the adjustable heating power and a controllable nitrogen gas flow rate it will be possible to set the RFQ inlet and outlet temperatures in the range of $(35\text{-}25)^0$ C thus not affecting dangerously the Inconel seals. We know from the past experience that RFQ was exposed even to a wider temperature range ($(10 - 35)^0$ C). The purging periods should be no less than 5 days followed by 2 days of pumping. The status of water out-gassing rate will be monitored using both the H_2O partial pressure and the ratio of H_2O/ H_2 as measured by the RGA during the vacuum periods. Once the H_2O/ H_2 ratio gets stabilized it will signal the limit of this heating method. On may expect this to occur at no less than after some (3-6) weeks of the continual heating operation.

For the SS heater method we assume the temperature rise from 20^0 C to 70^0 C with full RFQ body wrap, and from 20^0 C to 35^0 C with a partial wrap. As the RFQ copper body mass is about 700 kg it takes 13.5 MJ of energy to raise RFQ temperature by 50^0 C:

$$Q = 0.385 \text{ J/g-K} \times 50 \text{ K} \times 7\ 10^5 \text{ g} = \sim 13.5 \text{ MJ} \qquad (24)$$

and ~ 4 MJ to raise it by 15^0 C. The heat transfer from the tape to the RFQ body is no more than 25% effective so the required power over 3 hour period is 5 kW for 50^0 C (eq. 25) and 1.5 kW for 15^0 C temperature rise.

$$P = 100\% / 25\% \times 13.5 \text{ MJ} / 10.8 \times 10^3 \text{ s} = 5 \text{ kW} \qquad (25)$$

The outer circumference of RFQ body is ~ 85 cm and its length is 300 cm. For a full body heating we assume 50% of RFQ surface is covered with the heating tape. For this analysis we choose 0.5 mm thick and 2 cm wide SS tape leading to 75 wraps around the RFQ body with total tape length of 63.75 m. With a typical 72 10^{-6} Ω-cm resistivity of the 304 stainless steel the total heating tape resistance is then:

$$R = 72\ 10^{-6}\ \Omega\text{-cm} \times 6375 \text{ cm} / 0.1 \text{ cm}^2 = 4.6\ \Omega \qquad (26)$$

The required heating tape ac power supply current is then:

$$I = 1.66 \times [5000 \text{ W} / (4.6\ \Omega \times 10.8\ 10^3 \text{ s})]^{1/2} = 0.5 \text{ A} \qquad (27)$$

and the power supply power is (110 V x 0.5 A) x 1.66 = ~ 100 W. Consequently for the partial RFQ body heating the required power is only ~ 30 W. With such a low both voltage and current the heating tape will be wrapped with only 2 layers of 0.005" kapton tape to provide the electrical isolation from the RFQ body.

We should point-out that application of the heating tapes is much more practical and the heating is better controllable than with the hot nitrogen gas purge. In addition, the heating tape method can be applied while the RFQ is under vacuum permitting continuous monitoring of progress in both the vacuum level (Ion Gauge), and the ratio of Hydrogen to water (RGA).

9. Spill of hydrogen gas into RFQ vacuum space

In proton source operations hydrogen gas is continually fed into the plasma chamber, and its flow rate is adjusted to keep the hydrogen pressure at (50 – 100) mTorr. As only a minute fraction of this gas is actually converted to positive ions a set of three turbo pumps of 2700 L/S total pumping speed is mounted around the accelerating column to remove the bulk of the excess gas. Another turbo pump of 200 L/S pumping speed is mounted at the LEBT section. At 100 mTorr pressure in the ion source plasma chamber the vacuum level in the LEBT section is ~ 4 10^{-6} Torr. The measured vacuum level outside the RFQ vanes space is ~ 1.2 10^{-7} Torr at the LEBT connection end but at the exit of the RFQ it is ~ 3 10^{-8} Torr. This indicates existence of even more significant pressure gradient along the RFQ beam path which is inside the vanes space where most of the hydrogen gas is spilled. Below we consider option to minimize the pressure gradient by modifying the RFQ vessel flange connecting to LEBT. In figure 16 we show the vacuum connection between the LEBT exit beam pipe and the RFQ vacuum space. The RFQ entrance orifice is 9.5 mm in diameter and 17.46 mm in length giving a conductance for H_2 gas at 5.8 L/S. There is, however, a 0.8 mm space between the vacuum and the vanes

flanges at a circumference of 125.6 mm giving a surface area of ~ 100 mm^2 for the gas flow there. As the cross-section area of the orifice is ~ 70 mm^2, only 42% of hydrogen from LEBT will pass through the orifice, and so the H_2 spill rate into the inner space of the vanes is: 0.42 x 4 10^{-6} Torr x 5.8 L/S = 9.8 10^{-6} Torr-L/S. If this gas spill was uniformly distributed along the entire length of the vanes (as the out-gassing is) it would be pumped out at 1479 L/S (Table 4) leading to a partial pressure of 6.5 10^{-9} Torr. Unfortunately, this H_2 gas source is at the entrance to the RFQ, so the conductance is strongly suppressed along the vanes length, e.g. the area of the last slots will see only~6% of the hydrogen spill in the area of the first slot. Naturally, this leads to a gradient of H_2 pressure along the RFQ length with a projected pressure in the first 1/15th RFQ section to be ~10^{-7} Torr. This LEBT induced partial pressure may be too high for the proper RFQ operations when contributions from the system out-gassing (and other sources) are added.

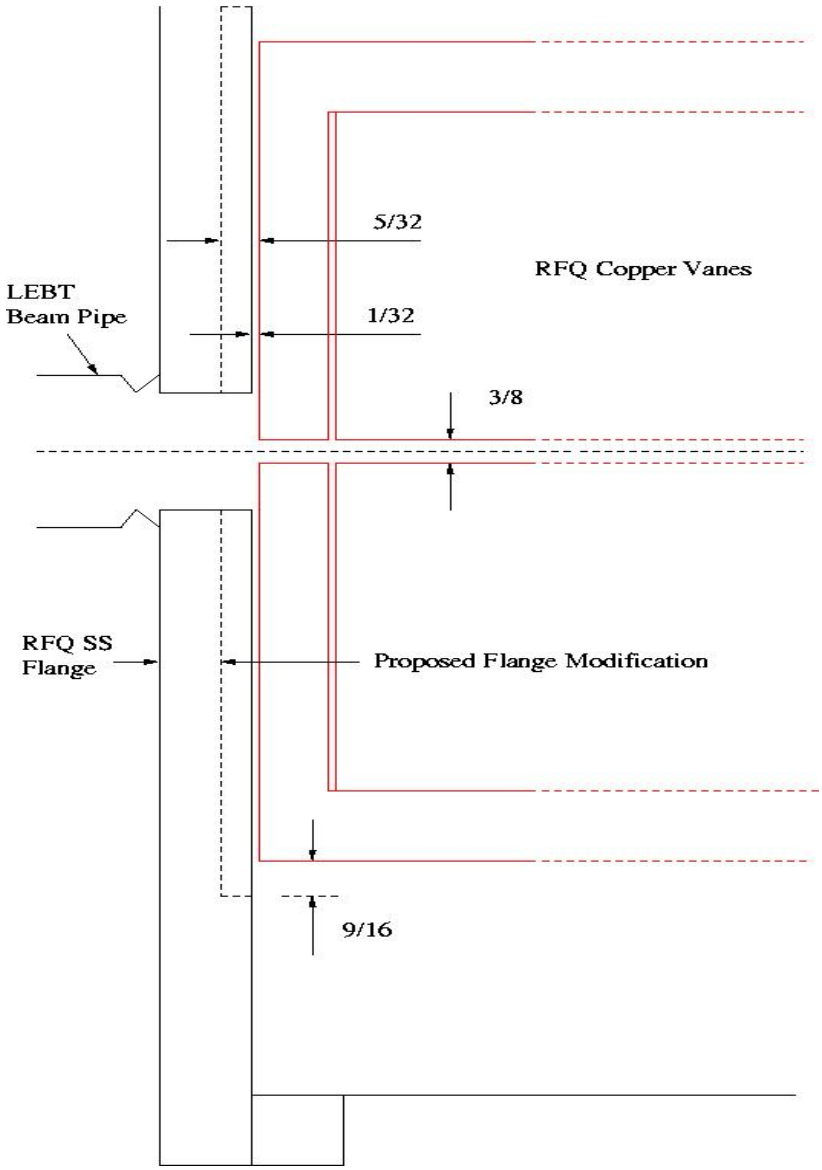

Fig. 14 Present arrangement and proposed modification of the RFQ vacuum vessel flange (dim. in inches)

A possible solution to this problem is shown in Fig. 14. We propose to make a circular, counter-board cut-out in the central portion of the SS flange. This will allow some 90% of LEBT hydrogen gas spill enter the outside space of the vanes where it will be pumped out at a higher speed. A fraction (~23%) of this gas, however, will be back-filled into the inner vanes space suppressing somewhat the expected gain. In figure 15 a comparison of

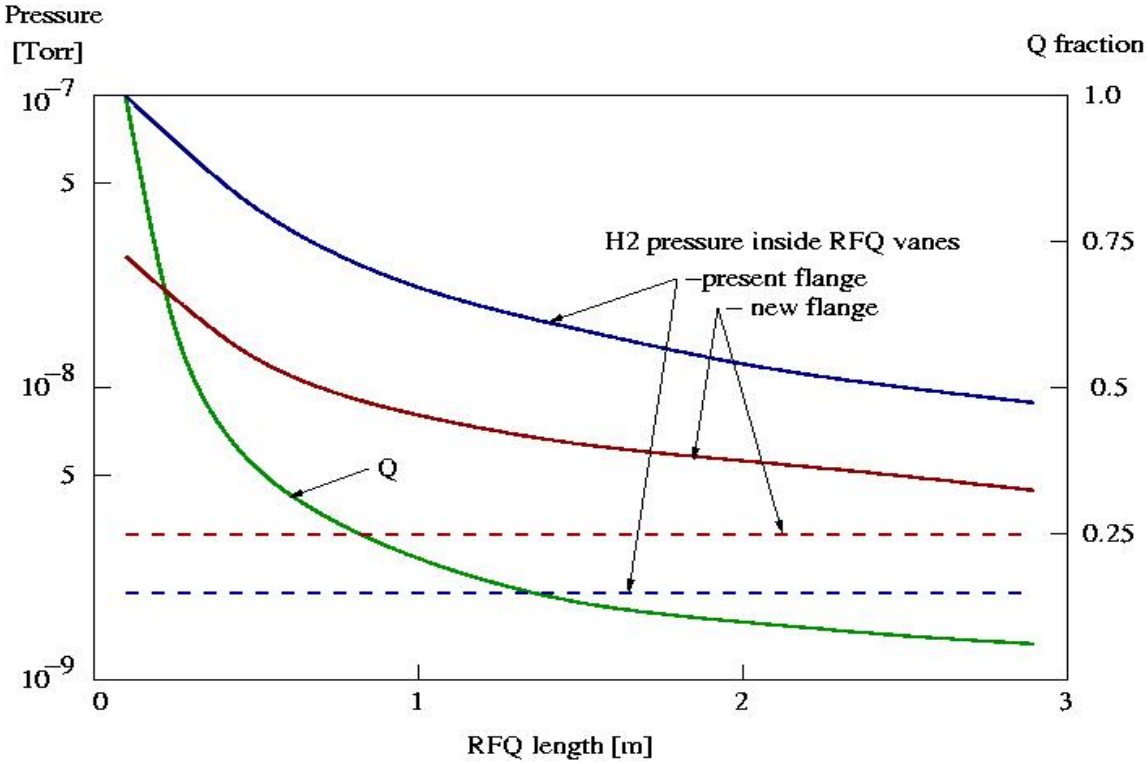

Fig. 15 Projected pressure profile of H_2 spill from LEBT into inner space of RFQ (Green line – fraction of hydrogen load Q, solid blue and brown lines - projections with present and proposed RFQ flange, respectively, dotted lines – partial pressure of H_2 backflow from the outer RFQ vacuum space)

the LEBT induced H_2 pressure expectations with the present and proposed arrangements of the RFQ flange is shown. A possible pressure suppression factor at the RFQ entrance is ~ 3.6, and ~ 2 at its exit.

The RFQ vacuum flange is large but it is used only in the 1 bar differential pressure range application, so the counter-board cut-out should not affect its required strength. The strength analysis should be done, however, and if necessary a set of few radial ribs could be welded-in. A better solution to the excess hydrogen flow into the RFQ space would be to install a restrictive orifice near the end of the LEBT beam pipe. In such a case the flow both inside and outside space of the RFQ vanes would be strongly suppressed. This option, however, requires knowledge of the beam phase space in the last section of the LEBT pipe to make sure that the beam intensity will not be reduced in the same time.

10.Vacuum properties and beam transmission in HINS RFQ

The RFQ vacuum level can be measured only outside the vanes space. Without the RF operation, but with the ion source H_2 gas pressure of ~ 100 mTorr, the vacuum level in the front part of the RFQ is ~ 1.5 E^{-7} Torr with water constituting ~ 30%, or 4 E^{-8} Torr, depending on the ambient temperature. With the RFQ operating at average power of ~ 600 W this pressure increases to ~ 3 E^{-7} Torr mostly due to the out-gassing water as observed in the RGA mass spectrum, and so the new water content is ~ 1.5 E^{-7} Torr. The analysis in Chapter 2 indicates that the vacuum level inside the vanes space is at least factor 2 higher than the one observed in the space outside the vanes. Consequently we should expect the out-gassing water to generate average pressure inside the vanes space in the range of ~ 3 E^{-7} Torr.

The ion gauges in HINS RFQ are far away from the inner space of the vanes so the measured pressure is averaged over a time needed to travel variety of molecular paths. In addition, the ion gauge response time is typically 100 ms, 30-100 times longer than the RFQ macro-pulse of (1-3) ms. Each RF pulse induced heating of the vane tips releases new batch of water molecules onto the surface. This generates in the space near the vanes tips an instantaneous pressure rise of up to ~ (30-100) x 3 E^{-7} = ~ (0.9 – 3) E^{-5} Torr. Such a pressure exceeds by order of magnitude the recommended pressure of E^{-6} Torr [11] for the RFQ operations. In addition, as described in Chapter 6, the high-voltage of RF pulse combined with high density of water molecules on the vanes surface leads to efficient formation of dual H_2O molecular clusters which break into the charged ions pairs. The $[H_3O]^+$ and $[OH]^-$ ions density increases through the entire RF macro-pulse forming effectively a "standing" cloud of ions in the vanes vacuum space. The beam particles may scatter more strongly on the charged ions than on the neutral H_2O molecules.

The above analysis shows that presence of the out-gassing water on the vanes surface, and consequently in the vanes vacuum space, will increase beam scattering and likely adversely affect the RFQ beam transmission. This conclusion is true for both the H^+ and H^- beams. In case of RFQ tests with the proton beam this situation is reinforced by the H_2 gas spill from the LEBT section. In summary, both the RF induced water vapor and the hydrogen spill should be suppressed as much as possible.

11. Effect of ambient temperature on the RFQ vacuum

We observe a strong dependence of the RFQ vacuum level with change of ambient temperature. The main reason is that the water vapor constitutes a dominant gas component in the RFQ vacuum space. The water molecules are chemisorbed to the metal surface, and their desorption rate from the surface is temperature dependent. The average length of time water molecule resides on the metal surface constitutes most important factor affecting the overall pumping speed. It turns out that the average residence time increases by some 10 orders of magnitude [3] between 450^0 C and 22^0 C. If the rate of the rise and/or fall of the residence time was independent of the temperature range than the residence time would be approximately changing by a factor of 10 per 40^0 C interval. This is not likely to be the case, however, for the temperature range closer to the freezing

point at 0^0 C when the water molecules will reside on the surface (for practical purpose) for an infinitive time. Scaling from the $(22 - 450)^0$ C temperature range, the rate of desorption would be slowed down by a factor of 5 between 30^0 C and 10^0 C. With the observed 2 10^{-7} Torr partial pressure of water in the RFQ outer vanes space at 30^0 C one should then expect "improvement" of the vacuum level down to about 4 10^{-8} Torr with the RFQ vessel external walls cooled down to10^0 C. The actually measured RFQ vacuum level at 10^0 C was found to be 1.5 10^{-8} Torr, nearly a factor 3 lower. We believe that the lower than expected vacuum level is possibly due to the acceleration of the residence time length as the surface temperature gets closer to 0^0 C. One may also anticipate that at lower temperatures, when the formation of multi-molecular layers is more likely to occur, there is an increase of absorption of water molecules on the in-homogeneous vacuum vessel inner surfaces. A typical residual gas mass spectrum of the RFQ vacuum taken at 12^0 C is shown in figure 15, and at about 24^0 C in figure 16. At lower temperature the

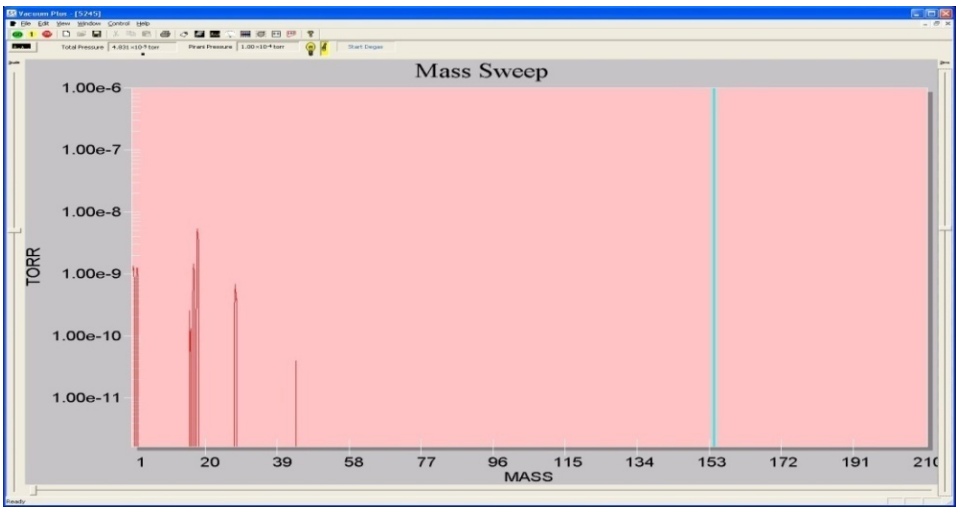

Fig. 15 Residual gas mass spectrum at 10^0 C

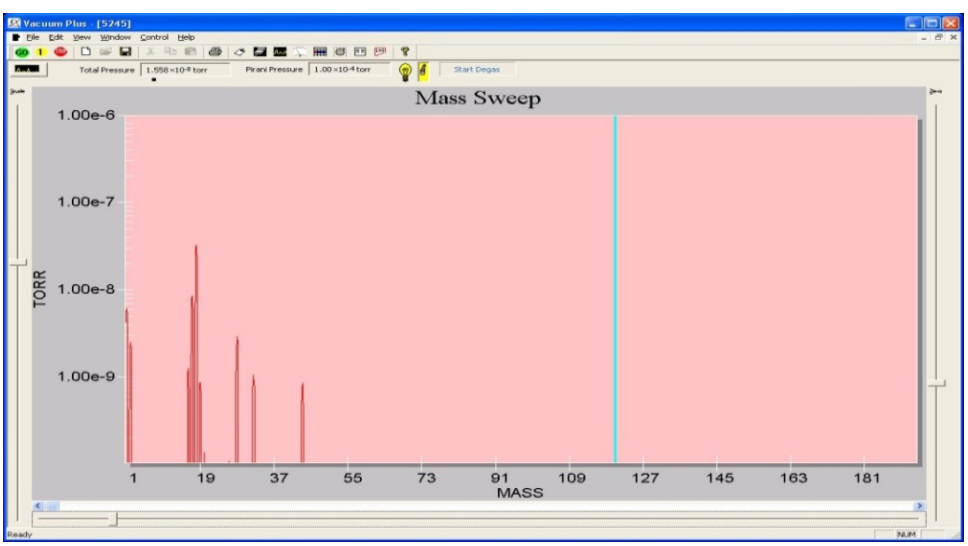

Fig. 16 Residual gas mass spectrum at 20^0

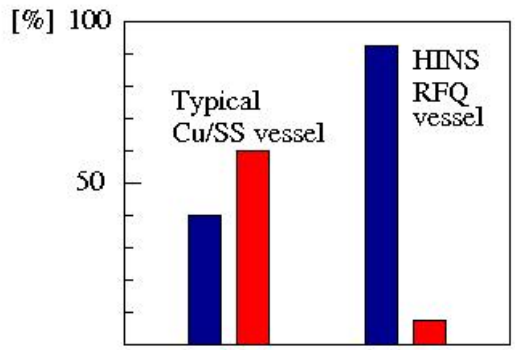

Fig. 17 H_2O (blue) and H_2 (red) fractions for a typical Cu/SS vessel and for HINS RFQ

partial pressure of water constitutes about 80% of all gas species, and at 24^0C partial pressure of water is about 94 % of all gas species. After 9 months of pumping of the RFQ vessel, one should expect hydrogen to be a dominant gas. A comparison of H2O and H2 fractions for a standard Cu/SS vessel to the HINS RFQ is shown in figure 17.

12. RFQ performance with repaired Inconel seal

In an effort to find all possible reasons for the resonant RF frequency decay in the HINS RFQ a physical inspection was made of the RFQ interior space. It was found that indeed one of the Inconel seals has buckled. After RFQ returned from the repair there was no observable change in its performance. The initial sparking at RF couplers area has continued and the forward RF power was frequently dropping off. After conditioning RFQ at a very low power for many days there was one successful measurement when the forward RF power remained constant for about 60 minutes (HINS logbook, Nov.4, 2009). This measurement was performed with a 1 ms pulse at 2 Hz repetition rate and the average RF power of 650 W. The data in figure 18 show only the forward power and do

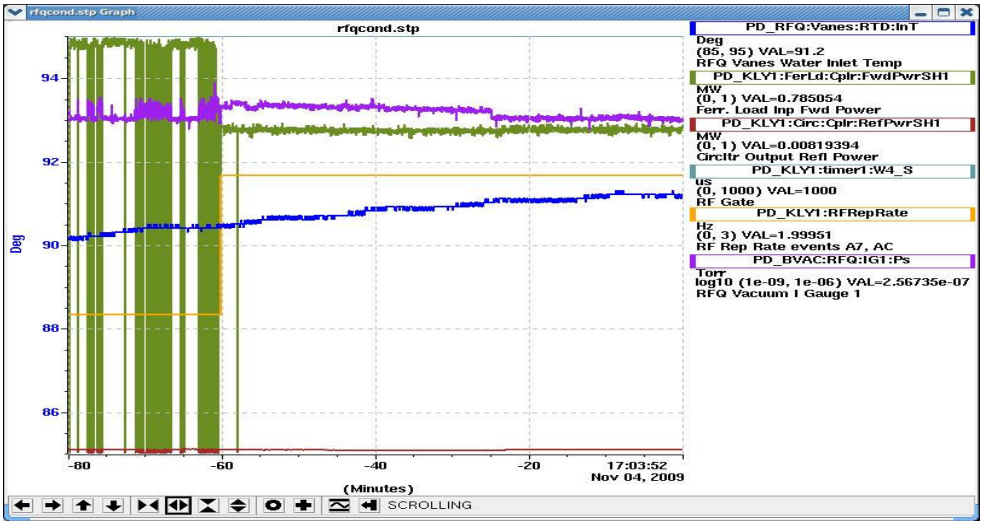

Fig. 18 RF forward power load (green) as a function of time for 650 W average power after seal repair.

not show the RF resonant frequency for this test. Consequently it is unknowable if the resonant frequency was actually constant in that test. In the pre-repair measurement with similar conditions (0.75 ms, 2 Hz, 600 W) the resonant frequency decay was observed after about 20 minutes of operation while the forward RF power remained constant for the duration of the test as shown in figure 19, (HINS logbook, Mar. 31, 2009). The lack of the RF frequency curve in figure 18 combined with the same response for the forward RF power in both tests does not allow us to conclude that the repair of the seal buckling had any effect on the RF resonant frequency response. This conclusion is consistent with two facts: (1) the seal is in the area of very low electric fields (less than few hundred volts/m as opposed to ~ 30 MV/m at the vanes tips) and (2) it is far away from the vane tips where the mechanical aberration would have an effect on the RF high voltage distribution. Consequently, it is difficult to devise a physics model explaining how the buckling of the seal would lead simultaneously to rapid vacuum rise and RF resonant frequency decay with the increase of RF power as described section 6.3.

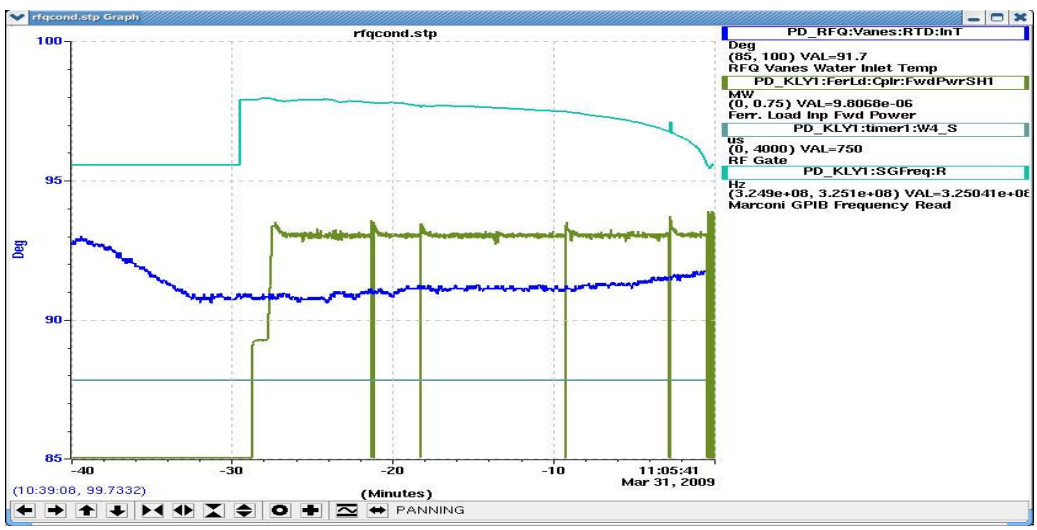

Fig. 19 RF forward power load (green) and RF frequency (light blue) as a function of time for 600 W of average power before seal repair

13.Recommendations for improvement of HINS RFQ

1st – Eliminate LCW manifold water leak into the RFQ vacuum space

Replace all Viton O- rings with the welded joints.

2nd – Decrease the ratio of out-gassing H_2O / H_2

Install SS tape heaters on the RFQ outer surface (or as very minimum set a hot nitrogen gas purging system to minimize the water out-gassing rate. Even if the two-part Inconel seals are not replaced with ones of a single length (and so only a moderate heating by (10-15) ^{0}C is allowed) using the tape heaters rather than a hot nitrogen purge is preferable as such a method offers faster and well controllable heating process.

3rd – Correct Inconel seals

Replace the 2-part Inconel seals with the single-piece seals to facilitate safe heating and cooling of the RFQ.

4th – Fix leaks and suppress discharges in the RF couplers

Replace all soldered joints with brazed or welded ones to suppress out-gassing of hydrocarbons and consequently the occurrence of sparking at the couplers.

5th - Lower the temperature of LCW cooling water in RFQ

Use chilled LCW water for cooling the RFQ vanes. This will help to minimize the out-gassing rate of water. In the APT/LEDA RFQ the LCW water inlet temperature is held at 50^0 F [10].

6th - Minimize H_2 and Cs gas spills into the RFQ vacuum space

Machine a counter-board cut-out in the flange connecting the RFQ vacuum shell with the LEBT beam pipe. This will allow redirect most of the ion source hydrogen and Cesium gas flows into the RFQ outer vacuum space minimizing in this way partial pressure of hydrogen in the beam path of the RFQ and also helping suppress the Cesium contamination of the RFQ vanes.

7th - *Stabilize the out-gassing rates and suppress HV discharges at the Ion Source*

Minimize the ambient temperature swings. In the warm vacuum system change of ambient temperature has considerable effect on the out-gassing rates. A standalone air conditioning comprising of both the chiller (for summer) and heater (for winter) in the area of the Ion Source, LEBT and RFQ would help to minimize temperature swings. The air conditioning would also stabilize the Ion Source operations as its electronics is residing at 50 kV potential.

14.Summary and conclusions

We presented a model of the RFQ vacuum system which reasonably reproduces the measured vacuum levels as a function of the ambient temperature as well as with the hydrogen spill from the LEBT section. The analysis of the Helium Leak Detector data agrees well with the predictions based on the known permeation factors for helium, air and water through the Viton seals. At low temperature (~10^0 C) water constitutes ~ 80% and hydrogen ~ 13% of all gas species detected in the outer space of the vanes but the relative water content increases to ~ 90% at ~ 20^0 C. After more than a year of pumping of the RFQ vessel, one should expect the ratio of partial pressure of water to hydrogen to be reversed. Our analysis shows, however, that the permeation of the LCW water through the Viton O-rings constitutes a continuing source of water vapor inside the RFQ vacuum space leading to the saturation of RFQ vanes surfaces with water molecules in spite of the continued pumping. In the absence of pumping the water vapor condensates

on the walls of RFQ vacuum vessel which are colder than the RFQ vanes structure which is held at ~ 10^0 C higher than the ambient temperature by the warm LCW water.

We also presented a model in which the RF power induced water out-gassing from the surface of the vanes tips combined with the applied high electric field across the vanes gap leads to generation of parasitic current of $[OH]^-$ ions. The model specifically shows that the rapid onset time for the run-away RF resonant frequency coincides with the rapid vacuum level rise, as indeed observed. The model also indicates that it is not just the overall RFQ vacuum level but the H_2 / H_2O molecular ratio that gives rise to the parasitic currents. The good vacuum level but with a low H_2 / H_2O ratio will only delay the onset time for the resonant RF frequency rapid run-away.

The RF power heating induced instantaneous high-density of water vapor in the vanes vacuum space together with the "standing cloud" of the $[OH]^-$ ions increases the overall beam scattering strength blowing-up the beam phase space and suppressing the beam transmission. This effect is true for both the H^+ and H^- beams. It is important to point out that the reduction of the RF pulse repetition rate lowers the average power but the instantaneous power in the micro-pulse does not change. Consequently, the passing beam, which is accelerated only during the micro-pulse, is affected by the out-gassing water molecules even at low RF repetition rates. In recent attempts to accelerate the proton beam in the HINS RFQ while operating without the water cooling the average RF power was reduced to ~ 0.2% of its nominal 4.5 kW by suppressing the RF repetition rate from 2 Hz to 0.03 Hz. This arrangement naturally made the beam detection (and its evaluation) difficult. Nevertheless it was observed that the beam transmission was much below the expectation thus confirming validity of the above model.

A successful RFQ operation was achieved in [9] only after the RFQ body heating at 70^0 C and with a strong supporting pumping system [10, 11]. In the most recent KEK effort [12] there is also a plan for the RFQ body heating up to 70^0 C with use of a strong cryo-pumping system. Such heating and pumping arrangements aim primarily at long-term suppression of the out-gassing water from a greater depth of the RFQ vanes surface. By using only a hot nitrogen gas purge the RFQ operation will be improved but very long and repeatable applications are required.

We would like point-out that none of the up-to-date reported analyses of the RFQ performance problems has outlined a physics model describing how out-gassing water from the vanes surface may affect the most fundamental parameter of RFQ performance, such as resonant frequency fall, with continuing application of RF power. We believe that the model outlined in this note, where the water molecular clusters collected on the vanes tips due to out-gassing process induced by RF power break into pairs of charged ions under the high (MV/m) RF electric field and giving rise in this way to parasitic currents, provides a very compelling explanation. In addition, the instantaneous high density of the water vapor in the space between the vanes tips generated with each new RF pulse, will very strongly affect beam transmission through the RFQ.

References:

[1] A.W. Chao and M. Tigner, *Handbook of Accelerator Physics and Engineering,* ISBN - 9810235003, 1998

[2] T. Page, *RFQ Mechanical Design,* Private communication, 2009

[3] J.F. O'Hanlon, *A User's Guide to Vacuum Technology,* ISBN-0-47-81242-0, 1989

[4] R. Reid, *Vacuum Technology in Accelerators,* Cockcroft Institute Lectures, 2007

[5] P. Danielson, *Gas Loads and O-rings,* A Journal of Practical and Useful Vacuum Technology, www.vacuumlab.com, 2000

[6] T. Page, G. Romanov, *RFQ thermal analysis and frequency response,* HINS Meeting Presentation, December 17, 2008

[7] Jim Steimel, *RFQ Resonant Frequency Decay,* HINS Meeting, April 23, 2009

[8] V. Medvedev, C. Rothfuss, E. Stuve, *Ionization of Water in High Electric Fields at and near a Metal (Electrode) Surface,* Gordon Research Conference on Electrochemistry, Ventura, California, 14-19 January 2001

[9] A.P. Letchford et al., *Testing, Installation, Commissioning and First Operation of ISIS RFQ Pre-Injector Upgrade",* Proc. of 2005 PAC, Knoxville, Tennessee, 2005

[10] R. Floersch, G. Domer, *Resonance Control Cooling System for the APT/LEDA RFQ,* Accelconf.web.cern.ch/accelconf/98/PAPERS/TH4099.PDF

[11] S. Shen et al., *APT/LEDA RFQ Vacuum Pumping System,* Proc. Particle Accelerator Conference, New York, 1999, p. 1333-1335

[12] M. Yoshioka, *J-PARC Accelerator Status and Commissioning Plan,* PAC 2009